Effect of pasteurisation and foaming temperature on the physicochemical and foaming properties of nano-filtered mineral acid whey

Nanik Purwanti[a, b, *], Sean A. Hogan[a], Valentyn A. Maidannyk[a], Shane Mulcahy[c]

Eoin G. Murphy[a, *]

[a] Teagasc Food Research Centre, Moorepark, Fermoy, Co. Cork, Ireland P61C996

[b] Department of Mechanical and Biosystem Engineering, IPB University, P. O. BOX 220, Bogor 16002, Indonesia

[c] Arrabawn Co-Operative Society Ltd., Nenagh, Co. Tipperary, Ireland E45XP68

[*] Corresponding authors.

Teagasc Food Research Centre, Moorepark, Fermoy, Co. Cork, Ireland P61C996

E-mail addresses:

eoin.murphy@teagasc.ie (E. G. Murphy), nanik_purwanti@apps.ipb.ac.id (N. Purwanti)

Revised on 30 April 2022; Accepted on 1 May 2022

Purwanti, N., Hogan, S. A, Maidannyk, V. A., Mulcahy, S., & Murphy, E. G. (2022). Effect of pasteurisation and foaming temperature on the physicochemical and foaming properties of nano-filtered mineral acid whey. *International Dairy Journal*, 133, 105419. doi: 10.1016/j.idairyj/2022.105419

Effect of pasteurisation and foaming temperature on the physicochemical and foaming properties of nano-filtered mineral acid whey

Nanik Purwanti[a, b, *], Sean A. Hogan[a], Valentyn A. Maidannyk[a], Shane Mulcahy[c]

Eoin G. Murphy[a, *]

[a] Teagasc Food Research Centre, Moorepark, Fermoy, Co. Cork, Ireland P61C996

[b] Department of Mechanical and Biosystem Engineering, IPB University, P. O. BOX 220, Bogor 16002, Indonesia

[c] Arrabawn Co-Operative Society Ltd., Nenagh, Co. Tipperary, Ireland E45XP68

[*] Corresponding authors.

Teagasc Food Research Centre, Moorepark, Fermoy, Co. Cork, Ireland P61C996

E-mail addresses:

eoin.murphy@teagasc.ie (E. G. Murphy), nanik_purwanti@apps.ipb.ac.id (N. Purwanti)

Abstract

Foaming can pose a major challenge during processing of acid whey (AW). In this study, nano-filtered mineral AW was collected from a commercial plant before (AW_0) and after pasteurisation (AW_{past}, 75 °C – 15 s). Both AW samples were foamed at 21 °C and in addition, AW_{past} was foamed at 61 °C, corresponding to the temperature of in-plant foaming. Physicochemical, foaming, and surface properties of AW samples were compared. Foaming at 21 °C resulted in less pronounced foam characteristics for AW_{past} compared to AW_0. Pasteurisation was found not to significantly affect

Revised on 30 April 2022; Accepted on 1 May 2022

Purwanti, N., Hogan, S. A, Maidannyk, V. A., Mulcahy, S., & Murphy, E. G. (2022). Effect of pasteurisation and foaming temperature on the physicochemical and foaming properties of nano-filtered mineral acid whey. *International Dairy Journal*, 133, 105419. doi: 10.1016/j.idairyj/2022.105419

physicochemical properties, however, interfacial kinetics during foaming were altered, which affected foaming behaviour. Foaming of AW_{past} at 61 °C produced more stable, "dry" foams. FTIR spectra confirmed the influence of protein unfolding at elevated temperatures on foaming, which was reversible upon cooling. This is significant as it gives processors a mean of controlling foaming through temperature control, where possible.

Keywords: Acid whey; Foaming; Temperature; Stability

Revised on 30 April 2022; Accepted on 1 May 2022
Purwanti, N., Hogan, S. A, Maidannyk, V. A., Mulcahy, S., & Murphy, E. G. (2022). Effect of pasteurisation and foaming temperature on the physicochemical and foaming properties of nano-filtered mineral acid whey. *International Dairy Journal*, 133, 105419. doi: 10.1016/j.idairyj/2022.105419

1. Introduction

Foam is a colloidal dispersion produced by dispersing gas or atmospheric air in an aqueous continuous phase by various methods such as supersaturation, injection, and agitation (Walstra, 2003). For foam to form, a surfactant is required to lower the surface tension between the air and the aqueous phase, and to stabilize the foam; energy input is also required and should be sufficient to disrupt the air/water interface. Amongst food grade surfactants, proteins have been widely studied in various systems and there is good understanding of their interfacial stabilization mechanisms (Kralova & Sjöblom, 2009). Bovine whey proteins have been widely investigated for their emulsifying and foaming properties (Bals & Kulozik, 2003; Lajnaf et al., 2018; Lazidis et al., 2016; Marinova et al., 2009; Martin, Grolle, Bos, Stuart, & Van Vliet, 2002). About 70% of whey protein is composed of β-lactoglobulin (β-lg) and α-lactalbumin (α-la) (~ 50 and 20%, respectively), and these components are largely responsible for the emulsifying and foaming properties of whey and its derivatives (Tosi, Canna, Lucero, & Ré, 2007); although the minor whey proteins also contribute to foaming. For example, presence of proteose-peptone (PP) was reported to have a significant effect on foaming properties of whey (Innocente, Corradini, Blecker, & Paquot, 1998; Zhu & Damodaran, 1994a).

Many publications detail the foaming behaviour of individual whey proteins, particularly β-lg. Foaming capacity of β-lg was directly affected by reversible structural rearrangement of the protein, whereas, its foam stability was best correlated with surface hydrophobicity (Phillips, Hawks, & German, 1995). A later study showed that pressure resistance of a foam film stabilised by β-lg aggregates was one-tenth to

Revised on 30 April 2022; Accepted on 1 May 2022
Purwanti, N., Hogan, S. A, Maidannyk, V. A., Mulcahy, S., & Murphy, E. G. (2022). Effect of pasteurisation and foaming temperature on the physicochemical and foaming properties of nano-filtered mineral acid whey. *International Dairy Journal*, 133, 105419. doi: 10.1016/j.idairyj/2022.105419

94 one-fifth of a film stabilised by non-aggregated β-lg (Rullier, Axelos, Langevin, &
95 Novales, 2009). However, foams made using a mixture of β-lg aggregates and non-
96 aggregated β-lg were more stable than those made of non-aggregated β-lg alone
97 (Rullier, Axelos, Langevin, & Novales, 2010). A recent research demonstrated that β-
98 lg had better foam stability when in the form of fibrils as opposed to aggregates (Hu
99 et al., 2019). Many factors can affect protein properties at the air/water interface and
100 thus affect foaming; for example, adsorption of β-lg at air/water interface, its surface
101 pressure isotherm, and elasticity of the interfacial layer have been shown to be strongly
102 affected by presence of electrolytes (Ulaganathan, Retzlaff, Won, Gochev, Gehin-
103 Delval, et al., 2017; Ulaganathan, Retzlaff, Won, Gochev, Gunes, et al., 2017). Similar
104 factors play a key role in determining foam properties of whey protein isolate (WPI)
105 (Bals & Kulozik, 2003; Davis, Foegeding, & Hansen, 2004; Kella, Yang, & Kinsella,
106 1989; Mahmoudi, Gaillard, Boué, Axelos, & Riaublanc, 2010; Pernell, Luck,
107 Foegeding, & Daubert, 2002). In general, these studies emphasized the importance of
108 protein concentration, temperature treatment, pH and ionic strength on
109 physicochemical properties of the proteins which, in turn, govern behaviour at
110 air/water interface of WPI foams. A recent study also highlighted the importance of
111 lactose content, pH and a_w for the manufacture of WPI powders with good foaming
112 properties (Audebert et al., 2019). Whilst mechanisms governing foaming properties
113 of purified protein systems, such as β-lg and WPI, have been elucidated extensively,
114 foaming mechanisms for lower value, lower protein systems such as acid whey (AW)
115 and sweet whey (SW) remain relatively unreported. In the context of this study AW
116 refers to mineral acid whey, produced by addition of HCl to milk during production of

Revised on 30 April 2022; Accepted on 1 May 2022
Purwanti, N., Hogan, S. A, Maidannyk, V. A., Mulcahy, S., & Murphy, E. G. (2022). Effect of pasteurisation and foaming temperature on the physicochemical and foaming properties of nano-filtered mineral acid whey. *International Dairy Journal*, 133, 105419. doi: 10.1016/j.idairyj/2022.105419

117 sodium caseinate, as opposed to acid whey obtained through acidification with lactic
118 acid.

119 AW and SW represent a matrix where various components (proteins, lactose and
120 minerals) and various interactions thereof, can affect foaming behaviour. Therefore, it
121 is difficult to directly correlate well-established knowledge of foaming behaviour in
122 purified protein systems to AW or SW. Even in their raw forms, AW and SW have
123 different foaming properties. This may be attributed to their different compositions
124 although further studies are required to confirm this. In general, AW has lower level
125 of lactose but much higher mineral content, especially calcium (Ca), magnesium (Mg),
126 and phosphorus (P) than SW (Bhargava & Jelen, 1996; Nishanthi, Vasiljevic, &
127 Chandrapala, 2017). Fresh untreated mineral AW had higher foam capacity than fresh
128 untreated SW, whereas, heat treatment reduced foamability of SW significantly
129 (Lajnaf et al., 2018). The same study also showed that heating allowed AW to maintain
130 its ability in reducing air/water interfacial tension, which was not the case for SW.
131 However, further knowledge on foaming behaviour and properties of AW is not
132 available because its study is rare. AW is a co-product stream produced during acid-
133 coagulation of dairy products, which can pose technological problems, such as
134 separation efficiencies in membrane processing of AW due to the extent of Ca
135 complexation in AW (Chandrapala et al., 2015). Lower pH, protein, and lactose
136 content but higher Ca and P content, in comparison with SW, means AW can be harder
137 to process, especially during evaporation and drying (Dec & Chojnowski, 2006). On
138 an industrial scale, mineral AW is typically obtained after precipitation of casein at pH
139 4.6 (e.g., by concentrated hydrochloric acid (HCl)). Subsequently the stream may be

Revised on 30 April 2022; Accepted on 1 May 2022
Purwanti, N., Hogan, S. A, Maidannyk, V. A., Mulcahy, S., & Murphy, E. G. (2022). Effect of pasteurisation and foaming temperature on the physicochemical and foaming properties of nano-filtered mineral acid whey. *International Dairy Journal*, 133, 105419. doi: 10.1016/j.idairyj/2022.105419

pre-concentrated using nanofiltration. In such cases, total solids (TS) increases from ~5% to ~20% and certain amount of monovalent and divalent salts permeate through the membrane. The removal of salts through this process is important to keep ash content in the final whey powder low. After pH neutralization to 6.8 and pasteurisation, the whey stream is further concentrated by vacuum evaporation, cooled slowly under agitation to induce lactose crystallization, and then spray dried (Drapala et al., 2018).

For food applications, AW foaming properties may be desirable; in contrast, foaming during AW production poses a manufacturing challenge for the industry. Foaming which takes place during processing may lead to tank overflow and can significantly affect processing especially when highly stabile foams are produced. Anti-foaming agents are sometimes added but their presence can consequently affect foaming properties of AW powder. Therefore, this research was performed in order to a) better understand the mechanisms of foaming in nano-filtered mineral AW obtained from addition of HCl to skim milk and b) use this information to formulate improved control strategies. The effect of pasteurisation on foam stability was studied, along with increasing temperature (room temperature to 61 °C) which corresponded to the most significant occurrence of in-plant foaming. In addition, interfacial and physicochemical properties of the nano-filtered AW were analysed to determine the mechanisms by which foaming occurs during industrial AW processing.

2. Materials and Methods

2.1 Materials

Revised on 30 April 2022; Accepted on 1 May 2022
Purwanti, N., Hogan, S. A, Maidannyk, V. A., Mulcahy, S., & Murphy, E. G. (2022). Effect of pasteurisation and foaming temperature on the physicochemical and foaming properties of nano-filtered mineral acid whey. *International Dairy Journal*, 133, 105419. doi: 10.1016/j.idairyj/2022.105419

Nano-filtered mineral AW samples were collected from the processing line at Arrabawn Co-Operative Society Ltd., Nenagh, Co. Tipperary, Ireland. During processing, AW was nano-filtered to ~20% total solids at < 8°C followed by adjustment to pH ~6.8 using potassium hydroxide (KOH). Samples of this stream were taken before (AW_0) and after (AW_{past}) pasteurisation by a direct contact heater at 75(±2) °C for 15 s. Three batches of AW were sampled at three-day intervals from the 2nd until the 9th of December 2019 (late lactation period). The following chemicals: 8-anilino-1-naphthalenesulfonic acid (ANS), sodium azide (NaN_3), sodium phosphate dibasic dihydrate ($Na_2HPO_4.2H_2O$), sodium phosphate monobasic monohydrate ($NaH_2PO_4.H_2O$), acetonitrile HPLC grade, trifluoroacetic acid (TFA) HPLC grade, α-la from bovine milk (≥85%), β-lg from bovine milk (≥90%), acetic acid glacial 100% were purchased from Merck (Wicklow, Ireland). Sodium acetate was purchased from VWR International (Dublin, Ireland).

2.2 Compositional analysis of acid whey

Fat and moisture contents were analysed using a CEM SMART Trac II (CEM Corp., North Carolina, USA). Moisture content was also measured by a thermo-gravimetric method; approximately 5 g of each AW sample was weighed accurately on an aluminium dish and then placed in the oven at 105 °C for 270 min (Pereira et al., 2020). pH was measured using a pH meter (Mettler Toledo, Greifensee, Switzerland). Crude protein content was analysed using the Dumas combustion method (LECO Instruments, Chesire, UK). Ash content was analysed gravimetrically (TGA 701 Thermogravimetric Analyzer, LECO Instruments, Chesire, UK). Lactose

Revised on 30 April 2022; Accepted on 1 May 2022
Purwanti, N., Hogan, S. A, Maidannyk, V. A., Mulcahy, S., & Murphy, E. G. (2022). Effect of pasteurisation and foaming temperature on the physicochemical and foaming properties of nano-filtered mineral acid whey. *International Dairy Journal*, 133, 105419. doi: 10.1016/j.idairyj/2022.105419

was determined by difference, i.e., subtraction of the sums of the weight percentage of crude protein, fat, moisture and ash from the total weight percentage (BeMiller, 2010), assuming that lactose is the only carbohydrate in whey. Each batch of AW was analysed in triplicate. Prior to each analysis, samples were vortexed and stirred thoroughly to ensure homogeneity. Composition of AW_0 and AW_{past} is shown in Table 1.

[TABLE 1]

2.3 Mineral analysis

All three batches of AW samples were centrifuged at 5,000×*g* for 10 min at 4 °C to separate suspended materials from the supernatant. Analysis of mineral content in both precipitates and supernatants were performed by an external laboratory (F.B.A. Laboratories, Ltd., Co. Waterford, Ireland) using Inductively Coupled Plasma Mass Spectrometry (ICP – MS, Agilent 7700 Series, USA).

2.4 Foaming experiments

Foaming experiments were performed, at 21°C, immediately after collection of nano-filtered AW (AW_0 and AW_{past}) from the plant. Additionally, AW_{past} were heated to 61 °C to simulate the temperature at which foaming sporadically occurs in the industrial plant. AW_{past} (100 mL) was heated for 10 min in a water bath at 70 °C to reach a sample temperature of 61 °C (coded as $AW_{past,+}$) and this sample was immediately placed in a measuring cylinder, with internal diameter of 6 cm and height of 21.45 cm, where the foams were generated at 61 °C. Foams were generated from

Revised on 30 April 2022; Accepted on 1 May 2022
Purwanti, N., Hogan, S. A, Maidannyk, V. A., Mulcahy, S., & Murphy, E. G. (2022). Effect of pasteurisation and foaming temperature on the physicochemical and foaming properties of nano-filtered mineral acid whey. *International Dairy Journal*, 133, 105419. doi: 10.1016/j.idairyj/2022.105419

90 mL of sample using an air sparging method (Kamath, Huppertz, Houlihan, & Deeth, 2008; Lazidis et al., 2016; Tosi et al., 2007). Air was pumped through a cylindrical air stone (diameter 1.4 cm, length 2.4 cm), fixed at the bottom of the measuring cylinder, at a rate of 4.5 L/min for 20 s (sparging time, t_s). Foaming and its subsequent decay were recorded up to ~ 900 s, and images of the foams were captured using a dual 16 Mega Pixel (MP) (with f-stop (the ratio of the focal length divided by the opening size) f/1.7) + 5 MP (f/1.9) digital camera (Samsung-J810Y/DS). The foaming experiments were repeated twice for each batch of AW, including $AW_{past,+}$.

2.4.1 Image analysis

The videos and images were analysed using GIMP – GNU Image Manipulation Program (developed by University of Berkley, USA). A measurement tool in the program converts pixel unit of the image to physical unit of dimension (e.g., mm). Desaturation was applied using the GIMP software to replace colours with luminosity shade of grey. The ImageJ program (developed by the National Institutes of Health (NIH), USA) was used to measure average air bubble diameter (the mean air bubble size was taken from ~ 300 bubbles).

2.4.2 Determination of foaming properties

Foam capacity (*FC*) or overrun at the end of sparging and the maximum foam density (*MD*) were calculated according to Marinova et al. (2009) as follows:

$$FC = V_{foam0}/V_{gas} \quad (1)$$

Revised on 30 April 2022; Accepted on 1 May 2022
Purwanti, N., Hogan, S. A, Maidannyk, V. A., Mulcahy, S., & Murphy, E. G. (2022). Effect of pasteurisation and foaming temperature on the physicochemical and foaming properties of nano-filtered mineral acid whey. *International Dairy Journal*, 133, 105419. doi: 10.1016/j.idairyj/2022.105419

224 $$MD = V_{liq0}/V_{foam0} \quad (2)$$

225 where V_{foam0} (L) is the volume of foam at the end of sparging and V_{gas} (L) is the air
226 volume used to produce the foam. V_{gas} in this experiment was defined as the air flow
227 rate multiplied by sparging time, which was constant at 1.5 L. V_{liq0} (L) is the volume
228 of liquid entrapped in the foam at the end of sparging. This was obtained by subtracting
229 the volume of the remaining liquid at the bottom of the measuring cylinder after the
230 air sparging from the initial volume of sample (90 mL).
231 Foam stability (S) was defined as the time for half of the V_{liq0} to drain back down ($t_{liq1/2}$,
232 [s]) to the bottom of the cylinder and the total time required for foams to completely
233 collapse (t_{ef}, [s]). Both time parameters were observed from the videos obtained.

234 *2.5 Protein profiles*

235 Protein profiles of AW samples were determined using a reverse-phase HPLC
236 (1200 series, Agilent Technologies, USA). AW was diluted to 0.25% protein content
237 using 0.1 M acetate buffer (pH 4.6) and subsequently centrifuged at 20,000×g for 20
238 min at 4 °C. The supernatant was filtered using 0.2 µm PES membrane filter (Agilent
239 Captiva, USA) and injected onto a Zorbax 300SB-C18 column, 5 µm, 4.6 × 150 mm
240 (Agilent Technologies, USA). The aqueous running buffer was Milli-Q water
241 containing 0.1% TFA and the organic running buffer was acetonitrile containing 0.1%
242 TFA. The buffer was run in gradient mode with a flow rate of 0.5 mL/min. Sample
243 injection volume was 15 µL and the injection was performed in duplicate. Two protein
244 standards, i.e., β-lg (0.125 mg/mL – 2 mg/mL) and α-la (0.125 mg/mL – 1 mg/mL)
245 were also run through the column to build calibration curves. Peak areas at related

Revised on 30 April 2022; Accepted on 1 May 2022
Purwanti, N., Hogan, S. A, Maidannyk, V. A., Mulcahy, S., & Murphy, E. G. (2022). Effect of pasteurisation and foaming temperature on the physicochemical and foaming properties of nano-filtered mineral acid whey. *International Dairy Journal*, 133, 105419. doi: 10.1016/j.idairyj/2022.105419

retention times were integrated and quantified with the calibration curves to obtain the remaining native protein content in AW_0, AW_{past} and $AW_{past,+}$. The denaturation degree (DD, [%]) of acid whey represents remaining native protein content (mg/mL) relative to the initial protein content (mg/mL) (Bals & Kulozik, 2003), which is expressed in Eq. (3)

$$DD = \left(1 - \frac{\text{remaining native protein content}}{\text{initial protein content}}\right) \times 100 \quad (3)$$

2.6 Surface hydrophobicity

A fluorometric assay was applied using ANS according to the method of Murphy et al. (2015), with slight modification. All AW samples were diluted to final protein concentrations of 0 to 1 g/L in 20 mM phosphate buffer pH 7.0 with 0.05% sodium azide. A stock solution of 0.945 mM ANS was prepared in the same phosphate buffer using an amber bottle wrapped by aluminium foil to prevent light exposure. The hydrophobicity measurement was carried out using a Cary Eclipse Fluorescense Photometer (Agilent Technologies, USA). Excitation wavelength was set at 370 nm and emission wavelength was run from 400-600 nm. The excitation and emission slits were set at 5 nm and 10 nm, respectively. Medium voltage and medium scan speed were applied. The temperature chamber was set at 21 °C prior to measurement. 100 µL of ANS solution was added to 2 mL of protein dispersion in a four-clear-sided cuvette, mixed, and then kept in the dark for 15 min. The fluorescence intensity was measured from buffer-ANS (as the blank, F_0) and then the lowest to the highest protein concentration conjugated with ANS (F). Each batch of AW was measured in duplicate.

Revised on 30 April 2022; Accepted on 1 May 2022
Purwanti, N., Hogan, S. A, Maidannyk, V. A., Mulcahy, S., & Murphy, E. G. (2022). Effect of pasteurisation and foaming temperature on the physicochemical and foaming properties of nano-filtered mineral acid whey. *International Dairy Journal*, 133, 105419. doi: 10.1016/j.idairyj/2022.105419

The intensity for each dilution was obtained by calculating the area under the curve of intensity as a function of wavelength. The relative fluorescence intensity (RFI) of each protein dilution was defined as RFI = (F- F_0)/ F_0. The surface hydrophobicity was expressed as the slope obtained by plotting the protein concentration against RFI.

2.7 Fourier Transform Infrared Spectroscopy (FTIR)

The state of protein secondary structure in AW_0, AW_{past}, and $AW_{past,+}$ were probed using FTIR spectroscopy (Bruker Tensor 27, Bruker Optik GmbH, Germany) equipped with an attenuated total reflection BioATR cell II at 21 °C. Additionally, AW_{past} were also analysed at 35 °C and 61 °C in the cell to determine changes that occurred during heating. The temperature was controlled using a Haake DC30-K20 digital control water bath (Thermo Scientific, UK). Prior to analysis, all samples were kept in the fridge overnight to allow suspended materials to sediment and obtain a clear supernatant. Samples (20 µL) were scanned between 4,000 cm^{-1} and 900 cm^{-1} with an average of 120 scans at a resolution of 4 cm^{-1}. Milli-Q water was used for background readings and subtracted automatically. All spectra were analysed using Opus 7.5 software (Bruker Optik GmbH, Germany) with the following steps: atmospheric compensation for H_2O and CO_2, vector normalization, and Fourier-self deconvolution. The later step applied Lorentzian shape with bandwidth and noise reduction factors of 25.55 and 0.3, respectively, for the amide I band of proteins (1700-1600 cm^{-1}).

The underlying spectral changes as result of pasteurisation performed in the AW plant or additional heating were presented as percentage of area spectral differences. These areas were integrated along the average band positions associated with the

Revised on 30 April 2022; Accepted on 1 May 2022
Purwanti, N., Hogan, S. A, Maidannyk, V. A., Mulcahy, S., & Murphy, E. G. (2022). Effect of pasteurisation and foaming temperature on the physicochemical and foaming properties of nano-filtered mineral acid whey. *International Dairy Journal*, 133, 105419. doi: 10.1016/j.idairyj/2022.105419

secondary structures of proteins (Barth & Zscherp, 2002; Boye, Ismail, & Alli, 1996; Boye, Alli, & Ismail, 1997; Qi et al., 1997; Yang, Yang, Kong, Dong, & Yu, 2015). The area of spectral differences between AW_{past} and AW_0, both at 21 °C, were used to quantify effects of pasteurisation in the processing plant; the difference in area between AW_{past} at 21 °C and AW_{past} at 35 °C or AW_{past} at 61 °C were also used to quantify effects of additional heating on $AW_{past.}$ The area of a sample heated to 61 °C and cooled to 21 °C prior to analysis (AW_{past+}) was compared to AW_{past} (measured at 21 °C) in order to determine reversibility of changes. The area values were obtained using integrate function in OriginPro® 2021 software (demo version, OriginLab Corp., Massachusetts, USA), using y-axis of zero as the base of integration. The percentage of area spectral difference was calculated using Eq. (4). All FTIR analysis were done in duplicate for each batch of AWs.

$$\%\ change\ in\ spectral\ area = \left(\frac{Area\ of\ sample}{|Area\ of\ reference|} - 1\right) \times 100 \qquad (4)$$

2.8 Surface properties of acid whey

A pendant drop method was applied to measure dynamic surface tension γ(t) and surface dilatational properties of AW using an optical tensiometer (Attension Theta Flex, Biolin Scientific, Sweden) connected to OneAttention software v3.1. An air drop with a surface area of 12 mm^2 (equal to 4 μL of air) was formed through an inverted needle (needle gauge of 22G, 0.718 mm in diameter) plunged in an optical glass cuvette filled with AW diluted to 0.1% w/w (AW_0 or AW_{past}) in sodium phosphate buffer (20 mM, pH 6.8 ±0.05). Formation of the air drop was controlled by an

Revised on 30 April 2022; Accepted on 1 May 2022
Purwanti, N., Hogan, S. A, Maidannyk, V. A., Mulcahy, S., & Murphy, E. G. (2022). Effect of pasteurisation and foaming temperature on the physicochemical and foaming properties of nano-filtered mineral acid whey. *International Dairy Journal*, 133, 105419. doi: 10.1016/j.idairyj/2022.105419

automatic dispenser unit (C201, Biolin Scientific, Sweden); meanwhile, temperature of the diluted AW in the cuvette was controlled using a temperature-controlled water bath. The following measurements were performed at least in duplicate for each batch of AW.

2.8.1 Dynamic surface tension and interfacial adsorption

The dynamic surface tension $\gamma(t)$ was recorded for 900 s at 21±1 °C to mimic the temperature during the lower temperature foaming experiments. The $\gamma(t)$ of AW_{past} was also recorded at temperature of 35±1°C to observe the effect of elevated temperature. The 35 °C was the maximum temperature that allowed formation of a stable air bubble in whey solution during 900 s of recording. Above this temperature, the air bubble immediately detached from the needle tip. Based on $\gamma(t)$, adsorption kinetic constants of AW at the air/water interface were calculated. An overall adsorption process of proteins at the air/water interface takes place through three steps, i.e., (1) proteins migrate from the bulk phase to the region immediately below the air/water interface by diffusion or convection, (2) proteins adsorb and unfold at the interface and (3) conformational changes of proteins takes place in the adsorbed layer (Guzey, McClements, & Weiss, 2003; Graham & Phillips, 1979). The adsorption kinetics controlled by diffusion can be derived from the modified Ward and Tordai equation (Graham & Phillips, 1979; Ward & Tordai, 1946) (Eq. 5). This equation assumes that the protein migration is diffusion-controlled, there is no energy barriers for the proteins move to the interface, and there are no conformational changes of the proteins after adsorption (Guzey et al., 2003).

Revised on 30 April 2022; Accepted on 1 May 2022
Purwanti, N., Hogan, S. A, Maidannyk, V. A., Mulcahy, S., & Murphy, E. G. (2022). Effect of pasteurisation and foaming temperature on the physicochemical and foaming properties of nano-filtered mineral acid whey. *International Dairy Journal*, 133, 105419. doi: 10.1016/j.idairyj/2022.105419

$$\pi = 2C_0RT\left(\frac{Dt}{3.14}\right)^{1/2} \quad (5)$$

where π is surface pressure (mN/m), defined as $\pi = \gamma_0\text{-}\gamma$ with γ_0 is the surface tension in the absence of proteins (Guzey et al., 2003); C_0 is the initial protein concentration (mol/m^3) in the bulk phase, R is the gas constant (in J/mol·K), T is the absolute temperature (K), and D is the diffusion coefficient (m^2/s) that can be calculated by Stokes-Einstein formula. A linear fit obtained by plotting π against $t^{1/2}$ indicates that diffusion-controlled migration of the proteins to the interface and the slope represents the kinetics of diffusion (k_{diff}) (Baeza, Sanchez, Pilosof, & Patino, 2005; Niño, Sánchez, Ruíz-Henestrosa, & Patino, 2005).

Changes in π after the diffusion step were used to monitor adsorption of the AW into the surface and configurational re-arrangements of the adsorbed proteins, in which the rates of these processes can be analysed by the first-order equation (Graham & Phillips, 1979; Niño et al., 2005; Patino et al., 1999) (Eq. 6).

$$\ln\left(\frac{\pi_{ss}-\pi_t}{\pi_{ss}-\pi_0}\right) = -kt \quad (6)$$

where π_{ss}, π_0 and π_t are the surface pressure (mN/m) value at steady-state condition (π at 900 s was used in this research), at t = 0, and at any time, t (s), respectively. Two linear regions were usually obtained by plotting $\ln[(\pi_{900}\text{-}\pi_t)/(\pi_{900}\text{-}\pi_0)]$ against t, in which the first slope represents the rate of adsorption and unfolding ($k_{a/u}$) and the second slope represents the rate configurational re-arrangement of proteins at the adsorbed layer (k_{arr}) (Patino et al., 1999; Patino et al., 2007).

Revised on 30 April 2022; Accepted on 1 May 2022
Purwanti, N., Hogan, S. A, Maidannyk, V. A., Mulcahy, S., & Murphy, E. G. (2022). Effect of pasteurisation and foaming temperature on the physicochemical and foaming properties of nano-filtered mineral acid whey. *International Dairy Journal*, 133, 105419. doi: 10.1016/j.idairyj/2022.105419

352 2.8.2 Surface dilatational properties

353 Surface viscoelastic property of the adsorbed AW layer at air/water interface was
354 measured by inducing a controlled oscillation to an air drop and simultaneously
355 recording the change in the surface tension and the drop area. The bubble was
356 oscillated at a constant amplitude of 0.2, giving a maximum ratio between area of the
357 deformed interface (A) and area of the nondeformed interface (A_0) of about 2 %, and a
358 constant frequency of 50 mHz. Surface dilatational modulus |E|, which represent
359 viscoelasticity of foam lamellae, was calculated using OneAttention software v3.1.

360 *2.9 Statistical analysis*

361 The results of all analysis are presented as the mean value of all the three batches.
362 Paired-samples t-tests were performed to compare effects of in-plant heat treatment
363 (pasteurisation performed in the AW processing plant) and additional heating used to
364 elevate temperature during foaming on AW physicochemical and foaming properties.
365 The null hypothesis supposed no effects of in-plant heat treatment and additional
366 heating on AW. Normality tests using Skewness and Kurtosis, Shapiro-Wilk test, and
367 observing normal Q-Q plots were performed by SPSS, to check if each variable was
368 normally distributed.

369 **3. Results**

370 *3.1 Mineral profiles*

371 AW samples collected from the plant contained suspended materials, which
372 formed a sediment when stored under static conditions. Mineral contents in

Revised on 30 April 2022; Accepted on 1 May 2022
Purwanti, N., Hogan, S. A, Maidannyk, V. A., Mulcahy, S., & Murphy, E. G. (2022). Effect of pasteurisation and foaming temperature on the physicochemical and foaming properties of nano-filtered mineral acid whey. *International Dairy Journal*, 133, 105419. doi: 10.1016/j.idairyj/2022.105419

precipitates and supernatants are shown in Table 2. The primary mineral constituents in AW_0 and AW_{past}, ordered from highest to the lowest, were calcium (Ca), potassium (K), phosphorus (P), magnesium (Mg), sulphur (S) and sodium (Na), which are in agreement with other reports for acid whey (Chandrapala et al., 2015; Nishanthi, Chandrapala, & Vasiljevic, 2017; Talebi et al., 2019). Table 2 shows that Ca, P, and Mg in AW_0 were prone to precipitation. Meanwhile, K, S, and Na tended to be somewhat more soluble, with broadly similar proportions between supernatant and precipitate. Similar trends were observed in AW_{past} with slightly higher proportions of Ca and P in AW_{past} precipitate than in AW_0 precipitate. AW_{past} contained more minerals (p <0.05) in precipitate (78.3%) than AW_0 (76.7%).

[TABLE 2]

3.2. Foaming properties

The foaming properties of AW samples are shown in Table 3. The properties affected by a) sampling point within the plant (AW_0 and AW_{past}) and b) foaming temperature applied to AW_{past} (i.e., room temperature and temperature at which foaming occurs in the plant) are described in the following sub-sections.

3.2.1 Effect of in-plant sampling point on foaming at 21 °C

Air bubbles in foams produced from AW_0 and AW_{past} (foamed at 21 °C) were visually similar (Fig. 1a). Visual differences were observed after half the volume of entrapped liquid in the foam drained ($t_{liq1/2}$), i.e., at time 8.5 s and 8.17 s for AW_0 and AW_{past}, respectively (Fig. 1b). The shape and size of air bubbles in AW_0 at $t_{liq1/2}$ seemed

Revised on 30 April 2022; Accepted on 1 May 2022
Purwanti, N., Hogan, S. A, Maidannyk, V. A., Mulcahy, S., & Murphy, E. G. (2022). Effect of pasteurisation and foaming temperature on the physicochemical and foaming properties of nano-filtered mineral acid whey. *International Dairy Journal*, 133, 105419. doi: 10.1016/j.idairyj/2022.105419

394 to be similar to those in the fresh foams, meanwhile those in AW_{past} were bigger
395 compared to their fresh counterparts (Fig. 1b) due to coalescence. This may be as a
396 result of the large variation in bubble size observed for AW_{past} (Table 3) which had
397 bigger average size and larger variation compared to AW_0 (Rio & Biance, 2014).
398 Gravity-driven drainage and insufficient time for the AW protein to adsorb at the
399 interface may also play a role, i.e., the rate of adsorption and unfolding ($k_{a/u}$) in AW_{past}
400 was slower than in AW_0 (Table 5). Whilst the $t_{liq1/2}$ of AW_0 was not significantly
401 different to AW_{past} ($p > 0.05$), the time taken for AW_0 foams to collapse completely
402 (72.0 ± 25.2 s) was longer ($p < 0.05$) than that of AW_{past} foams (48.2 ± 19.1 s). Foam
403 capacity (*FC*) of AW_{past} was significantly ($p < 0.05$) lower than that of AW_0 (see Table
404 3). Higher *FC* of AW_0 compared to AW_{past} was confirmed by overrun rates. On
405 average, AW_0 foams were formed at a rate of 19.1 mL/s compared to 16.4 mL/s for
406 AW_{past}. Furthermore, *FC* data was well correlated with *MD*, i.e., AW_0 had higher *FC*
407 and lower *MD*, indicating a more aerated foam. It is interesting to note that while
408 AW_{past} foams had higher density, the average diameter of constituent air bubbles did
409 not vary significantly from AW_0.

410 **[FIGURE 1]**

411 **[TABLE 3]**

412 3.2.1 Effect of foaming temperature

413 Foaming the AW_{past} at 61 °C (here referred as $AW_{past,+}$) led to more stable foams
414 than at 21 °C. The fresh foams (Fig. 1a) had similar appearance to the subsequent

Revised on 30 April 2022; Accepted on 1 May 2022
Purwanti, N., Hogan, S. A, Maidannyk, V. A., Mulcahy, S., & Murphy, E. G. (2022). Effect of pasteurisation and foaming temperature on the physicochemical and foaming properties of nano-filtered mineral acid whey. *International Dairy Journal*, 133, 105419. doi: 10.1016/j.idairyj/2022.105419

half-drained foams (Fig. 1b). This was confirmed by foaming properties listed in Table 3. $AW_{past,+}$ foams had significantly longer $t_{liq1/2}$ than AW_0 and AW_{past} foams; meanwhile, the foams did not completely collapse within a reasonable time frame. About 25 – 33% of the initial volume of $AW_{past,+}$ foams was observed to remain in the foaming cylinder after several hours while the entrapped liquid had completely drained much earlier. Foaming of $AW_{past,+}$ also resulted in significantly higher *FC* than foaming of AW_{past} at 21 °C (Table 3) with smaller size of air bubbles, but the deviation was high ($p > 0.05$). Furthermore, the smaller size of air bubbles observed in $AW_{past,+}$ did not manifest as higher MD, i.e., the MD in $AW_{past,+}$ was lower than in AW_{past}.

3.3 Protein profiles of AW samples

Fig. 2 shows the native whey protein content in AW samples. Pasteurisation reduced the content of native α-la, β-lg, and other proteins but only affected α-la content significantly, however in numeric terms the loss of native α-la was small. Pasteurisation resulted in denaturation of 7.6% of α-la, 3.1% of β-lg, and 6.7% of other proteins originally present in unpasteurised whey (AW_0). Additional heating of AW_{past} to a final temperature of 61 °C during foaming ($AW_{past,+}$) did not significantly affect the native protein content. Overall, pasteurisation only led to denaturation of 4.7% of total protein originally present in AW_0, which was in keeping with studies investigating the effect of heating of whey proteins at 72–77 °C for few seconds (Bogahawaththa et al., 2017; Muuronen, Partanen, Heidebrecht, & Kulozik, 2021; Rynne, Beresford, Kelly, & Guinee, 2004).

[FIGURE 2]

Revised on 30 April 2022; Accepted on 1 May 2022
Purwanti, N., Hogan, S. A, Maidannyk, V. A., Mulcahy, S., & Murphy, E. G. (2022). Effect of pasteurisation and foaming temperature on the physicochemical and foaming properties of nano-filtered mineral acid whey. *International Dairy Journal*, 133, 105419. doi: 10.1016/j.idairyj/2022.105419

437 *3.4 Surface hydrophobicity*

438 Surface hydrophobicity of AW_{past} was slightly (~2%) higher than AW_0 but the
439 difference was not statistically significant (Fig. 3). Further exposure of AW_{past} to
440 additional heating prior to foaming ($AW_{past,+}$) significantly increased the surface
441 hydrophobicity ($p < 0.05$) at protein concentrations above 0.2 g/L. However, the
442 differences in surface hydrophobicity between AW_{past} and $AW_{past,+}$ was small and not
443 deemed important (~4%).

444 **[FIGURE 3]**

445 *3.5. FTIR*

446 Typical spectra of AW samples in the amide I region are depicted in Fig. 4. All
447 AW samples had similar and overlapping spectra, which made evaluation of the effects
448 of heat treatments challenging. For this reason, the area of spectral difference between
449 samples was used to describe changes due to heat treatments.

450 **[FIGURE 4]**

451 Data in Table 4 indicate that pasteurisation of AW led to a small reduction of
452 intramolecular β-sheets, which may have been expected to correspond to increased
453 intermolecular β-sheets. However, there were no positive area changes observed at
454 1616-1620 cm^{-1}, which usually indicates formation of intermolecular β-sheet. In fact,
455 in the current study, intermolecular β-sheets were shown to be drastically decreased (-
456 1,790%) after pasteurisation. Pasteurisation resulted in greater peak intensities

Revised on 30 April 2022; Accepted on 1 May 2022
Purwanti, N., Hogan, S. A, Maidannyk, V. A., Mulcahy, S., & Murphy, E. G. (2022). Effect of pasteurisation and foaming temperature on the physicochemical and foaming properties of nano-filtered mineral acid whey. *International Dairy Journal*, 133, 105419. doi: 10.1016/j.idairyj/2022.105419

associated with α-helices (1625-1655 cm^{-1}); β-turns (1659-1671 cm^{-1}) and random coils (1646-1650 cm^{-1}). These changes reflect increases in the absorbance of functional groups associated with the structural elements in question. This may have been a result of partial unfolding of globular whey proteins that allows more extensive C=O and C-N stretching and vibrational motions. To gauge the effect of temperature, AW_{past} were analysed at 35 °C and 61 °C by FTIR, and then compared with the spectra of AW_{past} measured at 21 °C. Table 4 shows that area of spectral differences of intramolecular β-sheets, intermolecular β-sheets at 1616-1620 cm^{-1}, α-helix, and random coils in AW_{past} decreased when spectra were collected at 35 °C. On the contrary, a slight increase in intermolecular β-sheets at 1684-1686 cm^{-1} was observed. When the spectra were collected at 61 °C, levels of β-turns, intermolecular β-sheets at 1684-1686 cm^{-1}, and α-helix were markedly higher, at the expense of intramolecular β-sheets, intermolecular β-sheets at 1616-1620 cm^{-1} and random coils. Such changes in structural elements are broadly in line with previous publication (O'Loughlin, Kelly, Murray, Fitzgerald, & Brodkorb, 2015). Enhancement of structural re-arrangement and intermolecular interactions at the expense of intramolecular β-sheets in AW_{past} was clearly observed by increasing temperature from 35 °C to 61 °C.

[TABLE 4]

Analysis of a AW_{past} sample which had been heated to 61 °C and then returned to 21 °C before FTIR analysis (i.e. $AW_{past,+}$, Table 4) showed that its spectra was quite similar to that of unheated AW_{past} and markedly different from samples analysed at 35 and 61 °C. This suggest structural changes brought about through heating were, to a

Revised on 30 April 2022; Accepted on 1 May 2022
Purwanti, N., Hogan, S. A, Maidannyk, V. A., Mulcahy, S., & Murphy, E. G. (2022). Effect of pasteurisation and foaming temperature on the physicochemical and foaming properties of nano-filtered mineral acid whey. *International Dairy Journal*, 133, 105419. doi: 10.1016/j.idairyj/2022.105419

large extent, reversible. Structural changes to whey proteins are generally reversible at low protein concentrations and if the denaturation temperature is not exceeded (Donovan & Mulvihill, 1987). Reversible changes to whey protein structure (predominantly β-lg) tend to occur at temperatures below that required to expose the free sulfhydryl (–SH) groups (normally buried in the hydrophobic core of the native protein), which would not be expected at the temperatures applied here, i.e., ≤ 61°C.

3.6. Surface properties

3.6.1 Dynamic surface tension and interfacial adsorption

The air drop produced during measurement of γ(t) is shown in Fig. 5a. AW_{past} contained suspended materials even at 0.1% w/w of protein content, which were not apparent in AW_0 at the same protein content. Fresh AW samples collected from the plant contained insoluble materials but those in AW_{past} were visually more obvious upon dilution to 0.1% w/w protein content. These materials were most visible when AW_{past} was measured at 35 °C. For operational reasons it was not possible to perform this analysis at > 35 °C.

[FIGURE 5]

The initial γ(t) of air/water interfaces at 21 °C was 57.38 mN/m in AW_0 (Fig. 5b). Pasteurisation of AW_0 (yielding AW_{past}) further reduced ($p < 0.05$) the inital γ(t) to 55.74 mN/m when it was measured at 21 °C. Although in-plant pasteurisation seemed to significantly affect the initial γ(t), the average γ(t) during the last 60 s (quasi-equilibrium region) for AW_0 and AW_{past} was the same statistically, i.e., 50.12 (±0.97)

Revised on 30 April 2022; Accepted on 1 May 2022
Purwanti, N., Hogan, S. A, Maidannyk, V. A., Mulcahy, S., & Murphy, E. G. (2022). Effect of pasteurisation and foaming temperature on the physicochemical and foaming properties of nano-filtered mineral acid whey. *International Dairy Journal*, 133, 105419. doi: 10.1016/j.idairyj/2022.105419

mN/m and 50.00 (±1.46) mN/m. Much lower γ(t) in this region was obtained when AW_{past} was measured at 35 °C, i.e., 46.03 mN/m. These data, however, cannot tell if there was a difference between adsorption kinetics of the AWs at the air/water interface and if the kinetics governed the observed foam properties. Therefore, π against $t^{1/2}$ and $\ln[(\pi_{900}-\pi_t)/(\pi_{900}-\pi_0)]$ against t were plotted to calculate adsorption kinetics of AWs based on Eq. (5) and (6).

[FIGURE 6]

Fig. 6a shows the average values of π as function of $t^{1/2}$ for AW_0, AW_{past}, both measured at 21 °C, and AW_{past} measured at 35 °C; from the data, a linear fit representing the rate of diffusion-controlled migration of proteins to the interface can be derived. To enable this, the initial value of π should be lower than 10 mN/m (Guzey et al., 2003; Miller, Fainerman, Wüstneck, Krägel, & Trukhin, 1998; Patino & Niño, 1999) , which was not the case for the plots depicted in Fig. 6a. Therefore, k_{diff} was estimated from the initial rate of change of π-$t^{1/2}$ (Zhou, Tobin, Drusch, & Hogan, 2021) and listed in Table 5. The estimated values of k_{diff} increased significantly from AW_0 to AW_{past} (21 °C). Increasing temperature of AW_{past} to 35 °C during measurement did not significantly increase the k_{diff}. After the migration period, the proteins would adsorb, unfold and conformationally rearrange at the interface. The kinetics of these phenomena ($k_{a/u}$ and k_{arr}) were derived from Fig. 6b. However, in the current study, a linear fit can only be derived for the first-order rate constant of adsorption and unfolding ($k_{a/u}$). A longer period of γ(t) monitoring would be required to capture the kinetics of configurational rearrangement (k_{arr}) at the interface but this was not possible

Revised on 30 April 2022; Accepted on 1 May 2022
Purwanti, N., Hogan, S. A, Maidannyk, V. A., Mulcahy, S., & Murphy, E. G. (2022). Effect of pasteurisation and foaming temperature on the physicochemical and foaming properties of nano-filtered mineral acid whey. *International Dairy Journal*, 133, 105419. doi: 10.1016/j.idairyj/2022.105419

522 with the set up used in this research. The values of $k_{a/u}$ decreased significantly from
523 AW_0 to AW_{past} (21 °C). The $k_{a/u}$ remained relatively constant when AW_{past} was
524 measured at 35 °C. It should be noted that the slopes derived from AW_{past} measured at
525 21 °C and 35 ° C were only an estimation because the scattered data meant obtaining
526 an R^2 was difficult.

527 **[TABLE 5]**

528 3.6.2 Surface dilatational properties

529 The changes in complex modulus |E| are depicted in Fig. 5c. The |E| values for all
530 samples are scattered between 20-40 mN/m with no statistical differences. It should
531 be highlighted that the oscillation of the air drop was started immediately after the drop
532 was formed. In this case, compression and expansion was applied on the air/water
533 interface even when the interface was not fully stabilized by the proteins. After 1000
534 s, |E| of AW_{past} measured at 35 °C started to clearly deviate from AW_0 and AW_{past}
535 measured at 21 °C and increased with time. Meanwhile, no difference of |E| was
536 observed between AW_0 and AW_{past} measured at 21 °C until the end of the
537 measurement. This was most likely attributed by low protein concentration adsorbed
538 at the interface, which rendered variations in |E| undetectable (Benjamin, 2000).

539 **4. Discussion**

540 *4.1 Effects of in-plant heat treatment*

Revised on 30 April 2022; Accepted on 1 May 2022
Purwanti, N., Hogan, S. A, Maidannyk, V. A., Mulcahy, S., & Murphy, E. G. (2022). Effect of pasteurisation and foaming temperature on the physicochemical and foaming properties of nano-filtered mineral acid whey. *International Dairy Journal*, 133, 105419. doi: 10.1016/j.idairyj/2022.105419

Pasteurisation of nano-filtered mineral AW significantly affected foaming properties in terms of t_{ef}, *FC* and *MD* as can be seen through comparison of AW_0 and AW_{past} values in Table 3. However, the underlying mechanism causing the difference in behaviour is not immediately obvious. It could be expected that protein denaturation and aggregation during heat treatment may have played a role; such heat induced changes to structure of whey proteins can improve foam stability to an extent, with excessive amounts contributing to reduced stability (Bals & Kulozik, 2003; Croguennec et al., 2006; Ibanoğlu & Karataş, 2001; Kella, Yang, & Kinsella, 1989; Lajnaf et al., 2018; Rullier, Axelos, Langevin, & Novales, 2010; Tosi et al., 2007; Zhu & Damodaran, 1994b). However, as could be expected for such a low intensity heat treatment (75 °C x 15 s), the level of heat induced denaturation observed here is small (< 5%, Fig. 1) compared to the studies cited above, for example, the degree of denaturation reported by Bals & Kulozik (2003) was > 70%. Therefore, it is unlikely that such small differences were the underlying mechanism for difference in fouling behaviour of AW_0 and AW_{past}. In addition, the difference in foaming behaviour after heating observed in this study contrasted with the publications cited, i.e., heat treatment of AW decreased *FC* and foam stability ($t_{liq1/2}$ and t_{ef}) rather than increased them. This also suggests degree of denaturation and aggregation was not the underlying mechanism.

The effect of in-plant pasteurisation on surface hydrophobicity was similar to the effect on degree of denaturation i.e., there was a small increase which was not significantly different (Fig. 3). The data on structural rearrangement (Table 4, AW_0 vs. AW_{past}, measured at 21°C) showed that there was some effect of pasteurisation

Revised on 30 April 2022; Accepted on 1 May 2022
Purwanti, N., Hogan, S. A, Maidannyk, V. A., Mulcahy, S., & Murphy, E. G. (2022). Effect of pasteurisation and foaming temperature on the physicochemical and foaming properties of nano-filtered mineral acid whey. *International Dairy Journal*, 133, 105419. doi: 10.1016/j.idairyj/2022.105419

564 temperature. Looking at the data in more detail, an increase in intermolecular β-sheets,
565 as generally reported for heated dairy systems, was not observed; in contrast, there was
566 a marked decrease in intramolecular β-sheet in AW_{past}. A decrease in intermolecular
567 β-sheets at 1618 cm^{-1} was previously reported during concentration of skim milk from
568 9% to 25% TS (Markoska, Huppertz, Grewal, & Vasiljevic, 2019). This may be
569 associated with a heat-induced shift in the monomer-dimer equilibrium of β-lg towards
570 the monomeric form. β-lg can exist as monomer, dimer or octamer depending on
571 protein variant, temperature, and pH. Several authors have also reported a shift towards
572 monomeric form upon heating (Aymard, Durand, & Nicolai, 1996; Cairoli, Iametti, &
573 Bonomi, 1994; Lefèvre & Subirade, 2000). A decreased in intermolecular β-sheets at
574 1619-1620 cm^{-1} was also reported for heat-treated (143 °C, 3s) deaminated milk;
575 whereas, a constant level of intermolecular β-sheets was observed in heat-treated milk
576 only (Grewal, Huppertz, & Vasiljevic, 2018). However, the significance of this
577 decrease in the context of this study remains unclear and should be further investigated.
578 The observed shift from β-sheet to α-helix indicated an intermediate structural state
579 between the ordered and fully unfolded states (Yang, Dunker, Powers, Clark, &
580 Swanson, 2001) was present after pasteurising the AW, but this apparently was not
581 sufficient to increase *FC* and foam stability.

582 Significant differences were observed between their interfacial properties of AW_0
583 and AW_{past}. Pasteurisation significantly reduced the initial γ(t) (Fig. 5b). This may be
584 attributed by faster diffusion-controlled migration rate of the proteins from the bulk
585 phase to the interface, as indicated by significantly higher k_{diff} value of AW_{past} than
586 AW_0 (Table 5). After aging the air/water interface for 900s, the γ(t) of AW_{past} and AW_0

Revised on 30 April 2022; Accepted on 1 May 2022
Purwanti, N., Hogan, S. A, Maidannyk, V. A., Mulcahy, S., & Murphy, E. G. (2022). Effect of pasteurisation and foaming temperature on the physicochemical and foaming properties of nano-filtered mineral acid whey. *International Dairy Journal*, 133, 105419. doi: 10.1016/j.idairyj/2022.105419

were similar, which indicated roughly similar amount of materials adsorbed at the interface (Martin et al., 2002). However, stabilization of the interface by AW_{past} was different compared to AW_0. The proteins in AW_{past} were significantly slower to adsorb and unfold at the interface, as indicated by the $k_{a/u}$ value, which is in line with other studies. The $k_{a/u}$ values of heat-treated WPI at any protein concentrations and pH were lower than those of unheated WPI because hydrophobic moieties might be limited for surface interactions due to their involvement in protein-protein interactions during heating (Zhou et al., 2021). Considering that denaturation level and surface hydrophobicity of AW_{past} and AW_0 were not significantly different to affect their interfacial behaviour, slow adsorption and unfolding of the AW_{past} at the interface might be contributed by insoluble materials which were more obvious than in AW_0, as shown in Fig. 5a. The insoluble materials observed in AW samples were most likely calcium phosphate (CaP) as indicated by Drapala et al., (2018). These insoluble materials may limit the penetration and anchoring process of the proteins at the interface (Damodaran & Song, 1988). As a consequence, it is likely that stabilization of the air/water interface could slow down, which subsequently resulted in lower *FC*, less stable foams, and bigger bubbles than in AW_0.

4.2 Effects of foaming temperature

Foaming AW_{past} at 61 °C ($AW_{past,+}$) resulted in the most stable foams. This is significant because the rationale for performing this research is foaming observed in the plant at this temperature. Foaming at elevated temperature has been previously reported in milk. A previous research has demonstrated that the time required for the

Revised on 30 April 2022; Accepted on 1 May 2022
Purwanti, N., Hogan, S. A, Maidannyk, V. A., Mulcahy, S., & Murphy, E. G. (2022). Effect of pasteurisation and foaming temperature on the physicochemical and foaming properties of nano-filtered mineral acid whey. *International Dairy Journal*, 133, 105419. doi: 10.1016/j.idairyj/2022.105419

609 foams to collapse to half of its original volume at 5 – 85 °C ranged from a few minutes
610 to several hours, depending on the types of milk (Kamath et al., 2008). Another study
611 reported a range from a few seconds to an hour for ultra-high temperature (UHT)
612 processed milk and pasteurised milk foamed at 5 – 60 °C (Oetjen, Bilke-Krause,
613 Madani, & Willers, 2014). However, such studies have not been reported in whey
614 system.

615 The stable foams produced by $AW_{past,+}$ were most likely a result of structural
616 rearrangement of the proteins at 61 °C. Phillips et al. (1995) reported an increase in
617 random coil, α-helix, and β-turn structures in β-lg solutions after whipping at 3 – 45
618 °C, which were associated with higher *FC* of β-lg solution. These unfolded structures
619 were reversible after the foam collapsed. AW_{past} measured at 61 °C (Table 4) showed
620 significant increases in intermolecular β-sheets at 1684-1686 cm^{-1}, α-helix and β-turns,
621 which were not observed when $AW_{past,+}$ was cooled and measured at 21 °C. This
622 confirms that structural reversibility took place when $AW_{past,+}$ was cooled down. When
623 the proteins unfolded at 61 °C, exposed hydrophobic moieties were likely responsible
624 for the highest *FC* in $AW_{past,+}$. Based on Fig. 3, the differences in surface
625 hydrophobicity between AW_{past} and $AW_{past,+}$ was ~4%. Although it was numerically
626 small, it should be noted that structural reversibility may also be a factor here, as
627 surface hydrophobicity was measured at 21 °C.

628 CaP becomes more insoluble with increasing temperature, therefore is likely to
629 have been present in larger quantities when AW_{past} was foamed at 61 °C. It is possible
630 that their presence at air/water interface would act as a Pickering-like effect mediator
631 working synergistically or antagonistically at the interface with the unfolded state of

Revised on 30 April 2022; Accepted on 1 May 2022
Purwanti, N., Hogan, S. A, Maidannyk, V. A., Mulcahy, S., & Murphy, E. G. (2022). Effect of pasteurisation and foaming temperature on the physicochemical and foaming properties of nano-filtered mineral acid whey. *International Dairy Journal*, 133, 105419. doi: 10.1016/j.idairyj/2022.105419

632 proteins at 61 °C. This is an interesting observation and further investigation of the
633 effect of precipitated salts on whey protein stabilised foams is planned.

634 Foaming at 61 °C resulted in the formation of dry foams. Dry foam is formed
635 when most of the entrapped liquid drains and the volume fraction of liquid in the
636 bubbles is less than 10% (Langevin, 2017). Dry foams produced by whey proteins was
637 previously described as formation of stiff and rigid foams obtained after excessive and
638 prolonged whipping (Kuehler & Stine, 1974). Dry foam was also defined as physically
639 containing little liquid and consisting of thin films (Weaire & Hutzler, 1999), stabilized
640 by disjoining pressures such as electrostatic repulsion, van der Waals attraction, and
641 steric/hydration forces (Aronson, Bergeron, Fagan, & Radke, 1994; Stubenrauch &
642 Miller, 2004). Unlike AW_0 and AW_{past} foams (both foamed at 21 °C), $AW_{past,+}$ foams
643 (foamed at 61 °C) appeared to meet the definitions of dry foam, i.e., the foams were
644 stiff and rigid, and most of the initial volume of the liquid had been recovered at the
645 bottom of the cylinder during the time of observation, which indicated that most of the
646 entrapped liquid had drained. This was confirmed by much shorter $t_{liq1/2}$ than t_{ef} in
647 $AW_{past,+}$ foams. This is a particularly interesting observation from a processing
648 perspective. On one hand, the drainage of a large degree of liquid from foams can be
649 seen as desirable as it allows most of the liquid to go forward to subsequent processing.
650 On the other hand, strong and persistent dry foams may be challenging to remove from
651 processing lines and it may not be possible to adequately separate the drained liquid
652 for further use.

653 **5. Conclusion**

Revised on 30 April 2022; Accepted on 1 May 2022
Purwanti, N., Hogan, S. A, Maidannyk, V. A., Mulcahy, S., & Murphy, E. G. (2022). Effect of pasteurisation and foaming temperature on the physicochemical and foaming properties of nano-filtered mineral acid whey. *International Dairy Journal*, 133, 105419. doi: 10.1016/j.idairyj/2022.105419

Heat treatment and foaming temperature of the AW were key determinants of foaming behaviour in industrial acid whey samples. Pasteurisation, as may have been expected, had minimal effect on levels of denaturation and surface hydrophobicity yet significantly affected foaming, i.e., production of less stable foams. It is also pertinent to note that the differences between pasteurised and unpasteurised data (i.e., denaturation and hydrophobicity) are small and not in line with the magnitude of the difference observed in foaming data. This seemed, to some extent, to be supported by air/water surface tension data. However, the underlying mechanisms for difference in foaming behaviour requires further elucidation. This is perhaps indicative of the complex nature of the acid whey system. In particular, the effects of insoluble materials, such as calcium phosphate and lactose on foaming properties should be further studied.

Reversible changes in secondary structure of whey proteins in AW were found to be the key determinant in foaming behaviour at higher temperatures. At temperatures below denaturation temperature, these changes were responsible for highly stable foams, which remain in place even after most of the liquid has drained. These “dry foams” represent a major challenge during processing; however, the work presented here suggests that lowering the temperature at the point where foaming takes place in the processing plant (if possible) can help to alleviate such issues. Overall, this work illustrates the foaming-related challenges associated with processing of nano-filtered AW, highlights the effects of heating and provides increased understanding of aeration behaviour in this complex, under-studied dairy stream.

Acknowledgement

Revised on 30 April 2022; Accepted on 1 May 2022
Purwanti, N., Hogan, S. A, Maidannyk, V. A., Mulcahy, S., & Murphy, E. G. (2022). Effect of pasteurisation and foaming temperature on the physicochemical and foaming properties of nano-filtered mineral acid whey. *International Dairy Journal*, 133, 105419. doi: 10.1016/j.idairyj/2022.105419

This research is performed under Marie Sklodowska-Curie Career-FIT Fellowship, Project Code MF20180049, organized by Enterprise Ireland. The project received funding from the European Union's Horizon 2020 research and innovation programme under the Marie Skłodowska-Curie grant agreement No. 713654.

References

Aronson, A. S., Bergeron, V., Fagan, M. E., & Radke, C. J. (1994). The influence of disjoining pressure on foam stability and flow in porous media. *Colloids and Surfaces A: Physicochemical and Engineering Aspects*, *83*(2), 109–120. https://doi.org/10.1016/0927-7757(94)80094-4

Audebert, A., Beaufils, S., Lechevalier, V., Le Floch-Fouéré, C., Saint-Jalmes, A., & Pezennec, S. (2019). How foam stability against drainage is affected by conditions of prior whey protein powder storage and dry-heating: A multidimensional experimental approach. *Journal of Food Engineering*, *242*, 153–162. https://doi.org/10.1016/j.jfoodeng.2018.08.029

Aymard, P., Durand, D., & Nicolai, T. (1996). The effect of temperature and ionic strength on the dimerisation of β-lactoglobulin. *International Journal of Biological Macromolecules*, *19*(3), 213–221. https://doi.org/10.1016/0141-8130(96)01130-0

Baeza, R., Sanchez, C. C., Pilosof, A. M. R., & Patino, J. M. R. (2005). Interactions of polysaccharides with β-lactoglobulin adsorbed films at the air-water interface. *Food Hydrocolloids*, *19*(2), 239–248. https://doi.org/10.1016/j.foodhyd.2004.06.002

Revised on 30 April 2022; Accepted on 1 May 2022
Purwanti, N., Hogan, S. A, Maidannyk, V. A., Mulcahy, S., & Murphy, E. G. (2022). Effect of pasteurisation and foaming temperature on the physicochemical and foaming properties of nano-filtered mineral acid whey. *International Dairy Journal*, 133, 105419. doi: 10.1016/j.idairyj/2022.105419

699 Bals, A., & Kulozik, U. (2003). Effect of pre-heating on the foaming properties of
700 whey protein isolate using a membrane foaming apparatus. *International Dairy*
701 *Journal*, *13*(11), 903–908. https://doi.org/10.1016/S0958-6946(03)00111-0
702 Barth, A., & Zscherp, C. (2002). What vibrations tell us about proteins. *Quarterly*
703 *Reviews of Biophysics*, *35*(4), 369–430.
704 https://doi.org/10.1017/S0033583502003815
705 BeMiller, J. N. (2010). Carbohydrate Analysis. In *Food Analysis* (4th ed., pp. 147–
706 177). https://doi.org/10.1007/978-1-4419-1478-1
707 Benjamin, J. (2000). *Static and dynamic properteis of proteins adsorbed at liquid*
708 *interfaces*. Wageningen University.
709 Bhargava, A., & Jelen, P. (1996). Lactose solubility and crystal growth as affected by
710 mineral impurities. *Journal of Food Science*, *61*(1), 180–184.
711 https://doi.org/10.1111/j.1365-2621.1996.tb14754.x
712 Bogahawaththa, D., Chandrapala, J., & Vasiljevic, T. (2017). Thermal denaturation of
713 bovine immunoglobulin G and its association with other whey proteins. *Food*
714 *Hydrocolloids*, *72*, 350–357. https://doi.org/10.1016/j.foodhyd.2017.06.017
715 Boye, J. I., Alli, I., & Ismail, A. A. (1997). Use of Differential Scanning Calorimetry
716 and Infrared Spectroscopy in the Study of Thermal and Structural Stability of α-
717 Lactalbumin. *Journal of Agricultural and Food Chemistry*, *45*(4), 1116–1125.
718 https://doi.org/10.1021/jf960360z
719 Boye, J. I., Ismail, A. A., & Alli, I. (1996). Effects of physicochemical factors on the
720 secondary structure of β-lactoglobulin. *Journal of Dairy Research*, *63*(1), 97–
721 109. https://doi.org/10.1017/s0022029900031575

Revised on 30 April 2022; Accepted on 1 May 2022
Purwanti, N., Hogan, S. A, Maidannyk, V. A., Mulcahy, S., & Murphy, E. G. (2022). Effect of pasteurisation and foaming temperature on the physicochemical and foaming properties of nano-filtered mineral acid whey. *International Dairy Journal*, 133, 105419. doi: 10.1016/j.idairyj/2022.105419

722 Cairoli, S., Iametti, S., & Bonomi, F. (1994). Reversible and irreversible modifications
723 of β-lactoglobulin upon exposure to heat. *Journal of Protein Chemistry*, *13*(3),
724 347–354. https://doi.org/10.1007/BF01901568
725 Chandrapala, J., Duke, M. C., Gray, S. R., Zisu, B., Weeks, M., Palmer, M., &
726 Vasiljevic, T. (2015). Properties of acid whey as a function of pH and
727 temperature. *Journal of Dairy Science*, *98*(7), 4352–4363.
728 https://doi.org/10.3168/jds.2015-9435
729 Croguennec, T., Renault, A., Bouhallab, S., & Pezennec, S. (2006). Interfacial and
730 foaming properties of sulfydryl-modified bovine β-lactoglobulin. *Journal of*
731 *Colloid and Interface Science*, *302*(1), 32–39.
732 https://doi.org/10.1016/j.jcis.2006.06.061
733 Damodaran, S., & Song, K. B. (1988). Kinetics of adsorption of proteins at interfaces:
734 role of protein conformation in diffusional adsorption. *Biochimica et Biophysica*
735 *Acta (BBA)/Protein Structure and Molecular*, *954*(C), 253–264.
736 https://doi.org/10.1016/0167-4838(88)90080-5
737 Davis, J. P., Foegeding, E. A., & Hansen, F. K. (2004). Electrostatic effects on the
738 yield stress of whey protein isolate foams. *Colloids and Surfaces B:*
739 *Biointerfaces*, *34*(1), 13–23. https://doi.org/10.1016/j.colsurfb.2003.10.014
740 Dec, B., & Chojnowski, W. (2006). Characteristics of acid whey powder partially
741 demineralised by nanofiltration. *Polish Journal of Food and Nutrition Sciences*,
742 *15/56*(Spec.Issue 1), 87–90.
743 Donovan, M., & Mulvihill, D. M. (1987). Thermal denaturation and aggregation of
744 whey proteins. *Irish Journal of Food Science and Technology*, *11*, 87–100.

Revised on 30 April 2022; Accepted on 1 May 2022
Purwanti, N., Hogan, S. A, Maidannyk, V. A., Mulcahy, S., & Murphy, E. G. (2022). Effect of pasteurisation and foaming temperature on the physicochemical and foaming properties of nano-filtered mineral acid whey. *International Dairy Journal*, 133, 105419. doi: 10.1016/j.idairyj/2022.105419

745 Drapala, K. P., Murphy, K. M., Ho, Q. T., Crowley, S. V., Mulcahy, S., McCarthy, N.
746 A., & O'Mahony, J. A. (2018). Short communication: Multi-component
747 interactions causing solidification during industrial-scale manufacture of pre-
748 crystallized acid whey powders. *Journal of Dairy Science*, *101*(12), 10743–
749 10749. https://doi.org/10.3168/jds.2018-14836
750 Girardet, J. M., Linden, G., Loye, S., Courthaudon, J. L., & Lorient, D. (1993). Study
751 of Mechanism of Lipolysis Inhibition by Bovine Milk Proteose-Peptone
752 Component 3. *Journal of Dairy Science*, Vol. 76, pp. 2156–2163.
753 https://doi.org/10.3168/jds.S0022-0302(93)77551-7
754 Graham, D. E., & Phillips, M. C. (1979). Proteins at liquid interfaces. I. Kinetics of
755 adsorption and surface denaturation. *Journal of Colloid And Interface Science*,
756 *70*(3), 403–414. https://doi.org/10.1016/0021-9797(79)90048-1
757 Grewal, M. K., Huppertz, T., & Vasiljevic, T. (2018). FTIR fingerprinting of structural
758 changes of milk proteins induced by heat treatment, deamidation and
759 dephosphorylation. *Food Hydrocolloids*, *80*, 160–167.
760 https://doi.org/10.1016/j.foodhyd.2018.02.010
761 Guzey, D., McClements, D. J., & Weiss, J. (2003). Adsorption kinetics of BSA at air-
762 sugar solution interfaces as affected by sugar type and concentration. *Food*
763 *Research International*, *36*(7), 649–660. https://doi.org/10.1016/S0963-
764 9969(03)00004-8
765 Hu, J., Yang, J., Xu, Y., Zhang, K., Nishinari, K., Phillips, G. O., & Fang, Y. (2019).
766 Comparative study on foaming and emulsifying properties of different beta-
767 lactoglobulin aggregates. *Food and Function*, *10*(9), 5922–5930.

Revised on 30 April 2022; Accepted on 1 May 2022
Purwanti, N., Hogan, S. A, Maidannyk, V. A., Mulcahy, S., & Murphy, E. G. (2022). Effect of pasteurisation and foaming temperature on the physicochemical and foaming properties of nano-filtered mineral acid whey. *International Dairy Journal*, 133, 105419. doi: 10.1016/j.idairyj/2022.105419

https://doi.org/10.1039/c9fo00940j

Ibanoğlu, E., & Karataş, Ş. (2001). High pressure effect on foaming behaviour of whey protein isolate. *Journal of Food Engineering*, *47*(1), 31–36. https://doi.org/10.1016/S0260-8774(00)00096-0

Innocente, N., Corradini, C., Blecker, C., & Paquot, M. (1998). Dynamic Surface Properties of the Proteose-Peptone Fraction of Bovine Milk. *Journal of Dairy Science*, *81*(7), 1833–1839. https://doi.org/https://doi.org/10.3168/jds.S0022-0302(98)75753-4

Kamath, S., Huppertz, T., Houlihan, A. V., & Deeth, H. C. (2008). The influence of temperature on the foaming of milk. *International Dairy Journal*, *18*(10–11), 994–1002. https://doi.org/10.1016/j.idairyj.2008.05.001

Kella, N. K. D., Yang, S. T., & Kinsella, J. E. (1989). Effect of Disulfide Bond Cleavage on Structural and Interfacial Properties of Whey Proteins. *Journal of Agricultural and Food Chemistry*, *37*(5), 1203–1210. https://doi.org/10.1021/jf00089a001

Kralova, I., & Sjöblom, J. (2009). Surfactants used in food industry: A review. *Journal of Dispersion Science and Technology*, *30*(9), 1363–1383. https://doi.org/10.1080/01932690902735561

Kuehler, C. A., & Stine, C. M. (1974). Effect of Enzymatic Hydrolysis on Some Functional Properties of Whey Protein. *Journal of Food Science*, *39*(2), 379–382. https://doi.org/10.1111/j.1365-2621.1974.tb02899.x

Lajnaf, R., Picart-Palmade, L., Cases, E., Attia, H., Marchesseau, S., & Ayadi, M. A. (2018). The foaming properties of camel and bovine whey: The impact of pH and

Revised on 30 April 2022; Accepted on 1 May 2022
Purwanti, N., Hogan, S. A, Maidannyk, V. A., Mulcahy, S., & Murphy, E. G. (2022). Effect of pasteurisation and foaming temperature on the physicochemical and foaming properties of nano-filtered mineral acid whey. *International Dairy Journal*, 133, 105419. doi: 10.1016/j.idairyj/2022.105419

heat treatment. *Food Chemistry*, *240*, 295–303. https://doi.org/10.1016/j.foodchem.2017.07.064

Langevin, D. (2017). Aqueous foams and foam films stabilised by surfactants. Gravity-free studies. *Comptes Rendus - Mecanique*, *345*(1), 47–55. https://doi.org/10.1016/j.crme.2016.10.009

Lazidis, A., Hancocks, R. D., Spyropoulos, F., Kreuß, M., Berrocal, R., & Norton, I. T. (2016). Whey protein fluid gels for the stabilisation of foams. *Food Hydrocolloids*, *53*, 209–217. https://doi.org/10.1016/j.foodhyd.2015.02.022

Lefèvre, T., & Subirade, M. (2000). Molecular differences in the formation and structure of fine-stranded and particulate β-lactoglobulin gels. *Biopolymers*, *54*(7), 578–586. https://doi.org/10.1002/1097-0282(200012)54:7<578::AID-BIP100>3.0.CO;2-2

Mahmoudi, N., Gaillard, C., Boué, F., Axelos, M. A. V., & Riaublanc, A. (2010). Self-similar assemblies of globular whey proteins at the air-water interface: Effect of the structure. *Journal of Colloid and Interface Science*, *345*(1), 54–63. https://doi.org/10.1016/j.jcis.2010.01.036

Marinova, K. G., Basheva, E. S., Nenova, B., Temelska, M., Mirarefi, A. Y., Campbell, B., & Ivanov, I. B. (2009). Physico-chemical factors controlling the foamability and foam stability of milk proteins: Sodium caseinate and whey protein concentrates. *Food Hydrocolloids*, *23*(7), 1864–1876. https://doi.org/10.1016/j.foodhyd.2009.03.003

Markoska, T., Huppertz, T., Grewal, M. K., & Vasiljevic, T. (2019). FTIR analysis of physiochemical changes in raw skim milk upon concentration. *Lwt*, *102*, 64–70.

Revised on 30 April 2022; Accepted on 1 May 2022
Purwanti, N., Hogan, S. A, Maidannyk, V. A., Mulcahy, S., & Murphy, E. G. (2022). Effect of pasteurisation and foaming temperature on the physicochemical and foaming properties of nano-filtered mineral acid whey. *International Dairy Journal*, 133, 105419. doi: 10.1016/j.idairyj/2022.105419

https://doi.org/10.1016/j.lwt.2018.12.011

Martin, A. H., Grolle, K., Bos, M. A., Stuart, M. A. C., & Van Vliet, T. (2002). Network forming properties of various proteins adsorbed at the air/water interface in relation to foam stability. *Journal of Colloid and Interface Science*, *254*(1), 175–183. https://doi.org/10.1006/jcis.2002.8592

Miller, R., Fainerman, V. B., Wüstneck, R., Krägel, J., & Trukhin, D. V. (1998). Characterisation of the initial period of protein adsorption by dynamic surface tension measurements using different drop techniques. *Colloids and Surfaces A: Physicochemical and Engineering Aspects*, *131*(1–3), 225–230. https://doi.org/10.1016/S0927-7757(97)00075-7

Murphy, E. G., Roos, Y. H., Hogan, S. A., Maher, P. G., Flynn, C. G., & Fenelon, M. A. (2015). Physical stability of infant milk formula made with selectively hydrolysed whey proteins. *International Dairy Journal*, *40*, 39–46. https://doi.org/10.1016/j.idairyj.2014.08.012

Muuronen, K., Partanen, R., Heidebrecht, H. J., & Kulozik, U. (2021). Effects of conventional processing methods on whey proteins in production of native whey powder. *International Dairy Journal*, *116*, 104959. https://doi.org/10.1016/j.idairyj.2020.104959

Niño, M. R. R., Sánchez, C. C., Ruíz-Henestrosa, V. P., & Patino, J. M. R. (2005). Milk and soy protein films at the air-water interface. *Food Hydrocolloids*, *19*(3), 417–428. https://doi.org/10.1016/j.foodhyd.2004.10.008

Nishanthi, M., Chandrapala, J., & Vasiljevic, T. (2017). Compositional and structural properties of whey proteins of sweet, acid and salty whey concentrates and their

Revised on 30 April 2022; Accepted on 1 May 2022
Purwanti, N., Hogan, S. A, Maidannyk, V. A., Mulcahy, S., & Murphy, E. G. (2022). Effect of pasteurisation and foaming temperature on the physicochemical and foaming properties of nano-filtered mineral acid whey. *International Dairy Journal*, 133, 105419. doi: 10.1016/j.idairyj/2022.105419

837 respective spray dried powders. *International Dairy Journal*, *74*, 49–56.
838 https://doi.org/10.1016/j.idairyj.2017.01.002
839 Nishanthi, M., Vasiljevic, T., & Chandrapala, J. (2017). Properties of whey proteins
840 obtained from different whey streams. *International Dairy Journal*, *66*, 76–83.
841 https://doi.org/10.1016/j.idairyj.2016.11.009
842 O'Loughlin, I. B., Kelly, P. M., Murray, B. A., Fitzgerald, R. J., & Brodkorb, A.
843 (2015). Concentrated whey protein ingredients: A Fourier transformed infrared
844 spectroscopy investigation of thermally induced denaturation. *International*
845 *Journal of Dairy Technology*, *68*(3), 349–356. https://doi.org/10.1111/1471-
846 0307.12239
847 Oetjen, K., Bilke-Krause, C., Madani, M., & Willers, T. (2014). Temperature effect
848 on foamability, foam stability, and foam structure of milk. *Colloids and Surfaces*
849 *A: Physicochemical and Engineering Aspects*, *460*, 280–285.
850 https://doi.org/10.1016/j.colsurfa.2014.01.086
851 Patino, J. M. R., Conde, J. M., Linares, H. M., Jiménez, J. J. P., Sánchez, C. C.,
852 Pizones, V., & Millán, F. R. (2007). Interfacial and foaming properties of
853 enzyme-induced hydrolysis of sunflower protein isolate. *Food Hydrocolloids*,
854 *21*(5–6), 782–793. https://doi.org/10.1016/j.foodhyd.2006.09.002
855 Patino, J. M. R., & Niño, M. R. R. (1999). Interfacial characteristics of food emulsifiers
856 (proteins and lipids) at the air-water interface. *Colloids and Surfaces B:*
857 *Biointerfaces*, *15*(3–4), 235–252. https://doi.org/10.1016/S0927-7757(99)00012-
858 6
859 Patino, J. M. R., Niño, M. R. R., & Sánchez, C. C. (1999). Adsorption of whey protein

Revised on 30 April 2022; Accepted on 1 May 2022
Purwanti, N., Hogan, S. A, Maidannyk, V. A., Mulcahy, S., & Murphy, E. G. (2022). Effect of pasteurisation and foaming temperature on the physicochemical and foaming properties of nano-filtered mineral acid whey. *International Dairy Journal*, 133, 105419. doi: 10.1016/j.idairyj/2022.105419

isolate at the oil-water interface as a function of processing conditions: A rheokinetic study. *Journal of Agricultural and Food Chemistry*, *47*(6), 2241–2248. https://doi.org/10.1021/jf981119i

Pereira, J. P. F., Melquíades, L. L., Stephani, R., de Oliveira, L. F. C., Perrone, Í. T., & de Carvalho, A. F. (2020). Effect of sodium citrate on lactose crystallization in concentrated whey. *International Journal of Dairy Technology*, 1–8. https://doi.org/10.1111/1471-0307.12700

Pernell, C. W., Luck, P. J., Foegeding, E. A., & Daubert, C. R. (2002). Heat-induced changes in angel food cakes containing egg-white protein or whey protein isolate. *Journal of Food Science*, *67*(8), 2945–2951. https://doi.org/10.1111/j.1365-2621.2002.tb08843.x

Phillips, L. G., Hawks, S. E., & German, J. B. (1995). Structural Characteristics and Foaming Properties of β-Lactoglobulin: Effects of Shear Rate and Temperature. *Journal of Agricultural and Food Chemistry*, *43*(3), 613–619. https://doi.org/10.1021/jf00051a011

Qi, X. L., Holt, C., Mcnulty, D., Clarke, D. T., Brownlow, S., & Jones, G. R. (1997). *Effect of temperature on the secondary structure of b-lg*. *346*, 341–346.

Rio, E., & Biance, A. L. (2014). Thermodynamic and mechanical timescales involved in foam film rupture and liquid foam coalescence. *ChemPhysChem*, *15*(17), 3692–3707. https://doi.org/10.1002/cphc.201402195

Rullier, B., Axelos, M. A. V., Langevin, D., & Novales, B. (2009). β-Lactoglobulin aggregates in foam films: Correlation between foam films and foaming properties. *Journal of Colloid and Interface Science*, *336*(2), 750–755.

Revised on 30 April 2022; Accepted on 1 May 2022
Purwanti, N., Hogan, S. A, Maidannyk, V. A., Mulcahy, S., & Murphy, E. G. (2022). Effect of pasteurisation and foaming temperature on the physicochemical and foaming properties of nano-filtered mineral acid whey. *International Dairy Journal*, 133, 105419. doi: 10.1016/j.idairyj/2022.105419

https://doi.org/10.1016/j.jcis.2009.04.034

Rullier, B., Axelos, M. A. V., Langevin, D., & Novales, B. (2010). β-Lactoglobulin aggregates in foam films: Effect of the concentration and size of the protein aggregates. *Journal of Colloid and Interface Science*, *343*(1), 330–337. https://doi.org/10.1016/j.jcis.2009.11.015

Stubenrauch, C., & Miller, R. (2004). Stability of foam films and surface rheology: An oscillating bubble study at low frequencies. *Journal of Physical Chemistry B*, *108*(20), 6412–6421. https://doi.org/10.1021/jp049694e

Talebi, S., Chen, G. Q., Freeman, B., Suarez, F., Freckleton, A., Bathurst, K., & Kentish, S. E. (2019). Fouling and in-situ cleaning of ion-exchange membranes during the electrodialysis of fresh acid and sweet whey. *Journal of Food Engineering*, *246*, 192–199. https://doi.org/10.1016/j.jfoodeng.2018.11.010

Tosi, E., Canna, L., Lucero, H., & Ré, E. (2007). Foaming properties of sweet whey solutions as modified by thermal treatment. *Food Chemistry*, *100*(2), 794–799. https://doi.org/10.1016/j.foodchem.2005.11.001

Ulaganathan, V., Retzlaff, I., Won, J. Y., Gochev, G., Gehin-Delval, C., Leser, M., Noskov, B. A., Miller, R. (2017). β-Lactoglobulin adsorption layers at the water/air surface: 1. Adsorption kinetics and surface pressure isotherm: Effect of pH and ionic strength. *Colloids and Surfaces A: Physicochemical and Engineering Aspects*, *519*, 153–160. https://doi.org/10.1016/j.colsurfa.2016.03.008

Ulaganathan, V., Retzlaff, I., Won, J. Y., Gochev, G., Gunes, D. Z., Gehin-Delval, C., Leser, M., Noskov, B. A., Miller, R. (2017). β-Lactoglobulin adsorption layers at

Revised on 30 April 2022; Accepted on 1 May 2022
Purwanti, N., Hogan, S. A, Maidannyk, V. A., Mulcahy, S., & Murphy, E. G. (2022). Effect of pasteurisation and foaming temperature on the physicochemical and foaming properties of nano-filtered mineral acid whey. *International Dairy Journal*, 133, 105419. doi: 10.1016/j.idairyj/2022.105419

the water/air surface2. Dilational rheologyEffect of pH and ionic strength. *Colloids and Surfaces A: Physicochemical and Engineering Aspects*, *521*, 167–176. https://doi.org/10.1016/j.colsurfa.2016.08.064

Walstra, P. (2003). Physical Chemistry of Foods. In *Marcel Dekkers, Inc.* (Vol. 85). https://doi.org/10.1016/s0308-8146(03)00246-2

Ward, A. F. H., & Tordai, L. (1946). Time-dependence of boundary tensions of solutions I. The role of diffusion in time-effects. *The Journal of Chemical Physics*, *14*(7), 453–461. https://doi.org/10.1063/1.1724167

Weaire, D., & Hutzler, S. (1999). *The Physics of Foams*. Oxford University Press.

Yang, J., Dunker, A. K., Powers, J. R., Clark, S., & Swanson, B. G. (2001). β-Lactoglobulin molten globule induced by high pressure. *Journal of Agricultural and Food Chemistry*, *49*(7), 3236–3243. https://doi.org/10.1021/jf001226o

Zhou, B., Tobin, J. T., Drusch, S., & Hogan, S. A. (2021). Dynamic adsorption and interfacial rheology of whey protein isolate at oil-water interfaces: Effects of protein concentration, pH and heat treatment. *Food Hydrocolloids*, *116* (January), 106640. https://doi.org/10.1016/j.foodhyd.2021.106640

Zhu, H., & Damodaran, S. (1994a). Proteose Peptones and Physical Factors Affect Foaming Properties of Whey Protein Isolate. *Journal of Food Science*, *59*(3), 554–560. https://doi.org/10.1111/j.1365-2621.1994.tb05560.x

Zhu, H., & Damodaran, S. (1994b). Heat-Induced Conformational Changes in Whey Protein Isolate and Its Relation to Foaming Properties. *Journal of Agricultural and Food Chemistry*, *42*(4), 846–855. https://doi.org/10.1021/jf00040a002

Revised on 30 April 2022; Accepted on 1 May 2022
Purwanti, N., Hogan, S. A, Maidannyk, V. A., Mulcahy, S., & Murphy, E. G. (2022). Effect of pasteurisation and foaming temperature on the physicochemical and foaming properties of nano-filtered mineral acid whey. *International Dairy Journal*, 133, 105419. doi: 10.1016/j.idairyj/2022.105419

FIGURE CAPTIONS

Figure 1. 2D-images of air bubbles in the fresh foam (a) and after half the volume of the entrapped liquid in the foam drained (b). The scale bar is 2 mm.

Figure 2. The remaining native α-la, β-lg, and other proteins in AW samples before pasteurisation (AW_0), after pasteurisation (AW_{past}) and after heat treatment at 61 °C ($AW_{past,+}$). * indicates a significant difference between the two AW samples ($p < 0.05$).

Figure 3. Relative fluorescence intensity (RFI) of AW as function of protein concentration. The degree of hydrophobicity is represented by the slope and * indicates a significant difference between AW samples.

Figure 4. FTIR spectra (Amide I region) following normalization and deconvolution.

Figure 5. Tensiometer images of the air drop in AW_0, AW_{past} and AW_{past} (35 °C) at 0.1% w/w protein content during measurement of dynamic surface tension at 21 °C (AW_0 and AW_{past}) and 35 °C (AW_{past}) (a), surface tension as a function of time (b) and dilatational modulus as a function of time (c).

Figure 6. The average of the square root of time ($t^{1/2}$) dependence of surface pressure (π) (a) and representative of fit of first-order rate constant of adsorption and unfolding (b).

Revised on 30 April 2022; Accepted on 1 May 2022
Purwanti, N., Hogan, S. A, Maidannyk, V. A., Mulcahy, S., & Murphy, E. G. (2022). Effect of pasteurisation and foaming temperature on the physicochemical and foaming properties of nano-filtered mineral acid whey. *International Dairy Journal*, 133, 105419. doi: 10.1016/j.idairyj/2022.105419

Table 1. Proximate composition of acid whey before (AW_0) and after pasteurisation (AW_{past}). Mean values ($\bar{x}$) and standard deviations (s) are expressed on a dry basis, except for the total solids. The statistical significance values (p) are also listed.

Sample	Total solids (%)			Proteins (%)			Fat (%)			Ash (%)			Lactose (%)		
	$\bar{x}$	s	p	$\bar{x}$	s	p	$\bar{x}$	s	p	$\bar{x}$	s	p	$\bar{x}$	s	p
AW_0	19.09	0.92	**0.11**	11.27	0.21	**0.51**	0.38	0.09	**0.15**	8.35	0.23	**0.93**	80.00	0.28	**0.74**
AW_{past}	18.78	0.94		11.20	0.34		0.42	0.06		8.35	0.24		80.03	0.38	

Revised on 30 April 2022; Accepted on 1 May 2022
Purwanti, N., Hogan, S. A, Maidannyk, V. A., Mulcahy, S., & Murphy, E. G. (2022). Effect of pasteurisation and foaming temperature on the physicochemical and foaming properties of nano-filtered mineral acid whey. *International Dairy Journal*, 133, 105419. doi: 10.1016/j.idairyj/2022.105419

Table 2. Average mineral composition in supernatant and precipitate of AW_0 and AW_{past}. The mineral content that was significantly affected by pasteurisation ($p < 0.05$) is marked *.

Mineral (mg/kg)	AW_0		AW_{past}	
	Supernatant	**Precipitate**	**Supernatant**	**Precipitate**
Calcium (Ca)	476.33*	10,308.00	529.33*	11,371.33
Potassium (K)	4,096.67	3,548.00	4,013.00	3,547.67
Phosphorus (P)	572.33	4,975.67	553.00	5,510.67
Magnesium (Mg)	187.00	588.00	187.67	652.00
Sulphur (S)	389.67	310.33	385.67	357.00
Sodium (Na)	365.67	272.00	354.33	286.67

Revised on 30 April 2022; Accepted on 1 May 2022
Purwanti, N., Hogan, S. A, Maidannyk, V. A., Mulcahy, S., & Murphy, E. G. (2022). Effect of pasteurisation and foaming temperature on the physicochemical and foaming properties of nano-filtered mineral acid whey. *International Dairy Journal*, 133, 105419. doi: 10.1016/j.idairyj/2022.105419

Table 3. Foaming properties of AW samples expressed as the mean value ($\bar{x}$) and standard deviation (s). The significance value (p) between AW_0 and $AW_{past,}$ both at 21 °C, or between AW_{past} at 21 °C and 61 °C (referred here as $AW_{past,+}$) for each variable is also listed.

Sample	$t_{liq1/2}$ (s)			t_{ef} (s)			*FC*			*MD*			*d* (µm)		
	$\bar{x}$	*s*	*p*	$\bar{x}$	*s*	*p*	$\bar{x}$	*s*	*p*	$\bar{x}$	*s*	*p*	$\bar{x}$	*s*	*p*
AW_0	8.50	5.61	**0.72**	72.00	25.18	***0.02***	0.25	0.04	***0.00***	0.15	0.01	***0.00***	1105.37	90.11	**0.96**
AW_{past}	8.17	5.53		48.17	19.14		0.22	0.05		0.18	0.02		1112.45	256.12	
$AW_{past,+}$	135.67	65.48	***0.00***	> 900	-	-	0.32	0.06	***0.00***	0.15	0.02	***0.01***	956.76	266.40	**0.47**

Italic numbers under *p* indicate a significant difference either between AW_0 and AW_{past} or between AW_{past} and $AW_{past,+}$.

$t_{liq1/2}$: the time for half volume of the entrapped liquid in the foams to drain back down.

t_{ef}: the total time required for foams to completely collapse.

FC: foam capacity

MD: the maximum foam density

d: diameter of air bubbles.

Revised on 30 April 2022; Accepted on 1 May 2022
Purwanti, N., Hogan, S. A, Maidannyk, V. A., Mulcahy, S., & Murphy, E. G. (2022). Effect of pasteurisation and foaming temperature on the physicochemical and foaming properties of nano-filtered mineral acid whey. *International Dairy Journal*, 133, 105419. doi: 10.1016/j.idairyj/2022.105419

Table 4. Summary of secondary structural changes in amide I proteins stated as area of the spectral difference (%).

Structure	Wavenumber (cm^{-1})	Reference (temperature)	Sample (temperature)	Reference (temperature)	Sample (temperature)	Reference (temperature)	Sample (temperature)	Reference (temperature)	Sample (temperature)
		AW_0 (21 °C)	AW_{past} (21 °C)	AW_{past} (21 °C)	AW_{past} (35 °C)*	AW_{past} (21 °C)	AW_{past} (61 °C)*	AW_{past} (21 °C)	$AW_{past,+}$ (21 °C)**
Intramolecular β-sheets	1627-1630	-6.2%		-3.9%		-15.1		-4.3%	
Intermolecular β-sheets	1616-1620	-1,792.0%		-57.4%		-388.8%		12.7%	
Intermolecular β-sheets	1684-1686	-0.8%		0.5%		22.6%		-3.0%	
α-helix	1652-1655	14.2%		-0.8%		6.5%		-5.4%	
Random coils	1646-1650	10.7%		-2.4%		-1.8%		-5.3%	
β-turns	1659-1671	23.0%		4.1%		74.1%		4.3%	

* These samples were AW_{past} that was analysed by FTIR at elevated temperatures (35 °C and 61 °C).

** This sample was AW_{past} that was subjected to additional heating to 61 °C as part of foaming experiments and then analysed by FTIR at 21 °C.

Revised on 30 April 2022; Accepted on 1 May 2022
Purwanti, N., Hogan, S. A, Maidannyk, V. A., Mulcahy, S., & Murphy, E. G. (2022). Effect of pasteurisation and foaming temperature on the physicochemical and foaming properties of nano-filtered mineral acid whey. *International Dairy Journal*, 133, 105419. doi: 10.1016/j.idairyj/2022.105419

Table 5. Dynamic parameters for diffusion, adsorption and unfolding of the AW_0 and AW_{past}.

Sample	Temperature (°C)	$k_{diff} \times 10^3$ ($mNm^{-1} s^{-0.5}$)	$k_{a/u} \times 10^3$ (s^{-1})	R^2
AW_0	21	20.56 (±2.07)*	3.63 (±0.77)*	0.825 (±0.10)
AW_{past}	21	22.62 (±2.03)	1.60 (±0.44)	−
AW_{past}	35	22.97 (±3.38)	1.53 (±0.54)	−

AW_0 is the AW before pasteurisation; droplet surface properties were measured at 21 °C

AW_{past} is the AW after pasteurisation, droplet surface properties were measured at 21 °C and 35 °C

k_{diff} is the kinetics of diffusion; $k_{a/u}$ is the rate of adsorption and unfolding; R^2 is the coefficient of determination.

Revised on 30 April 2022; Accepted on 1 May 2022
Purwanti, N., Hogan, S. A, Maidannyk, V. A., Mulcahy, S., & Murphy, E. G. (2022). Effect of pasteurisation and foaming temperature on the physicochemical and foaming properties of nano-filtered mineral acid whey. *International Dairy Journal*, 133, 105419. doi: 10.1016/j.idairyj/2022.105419

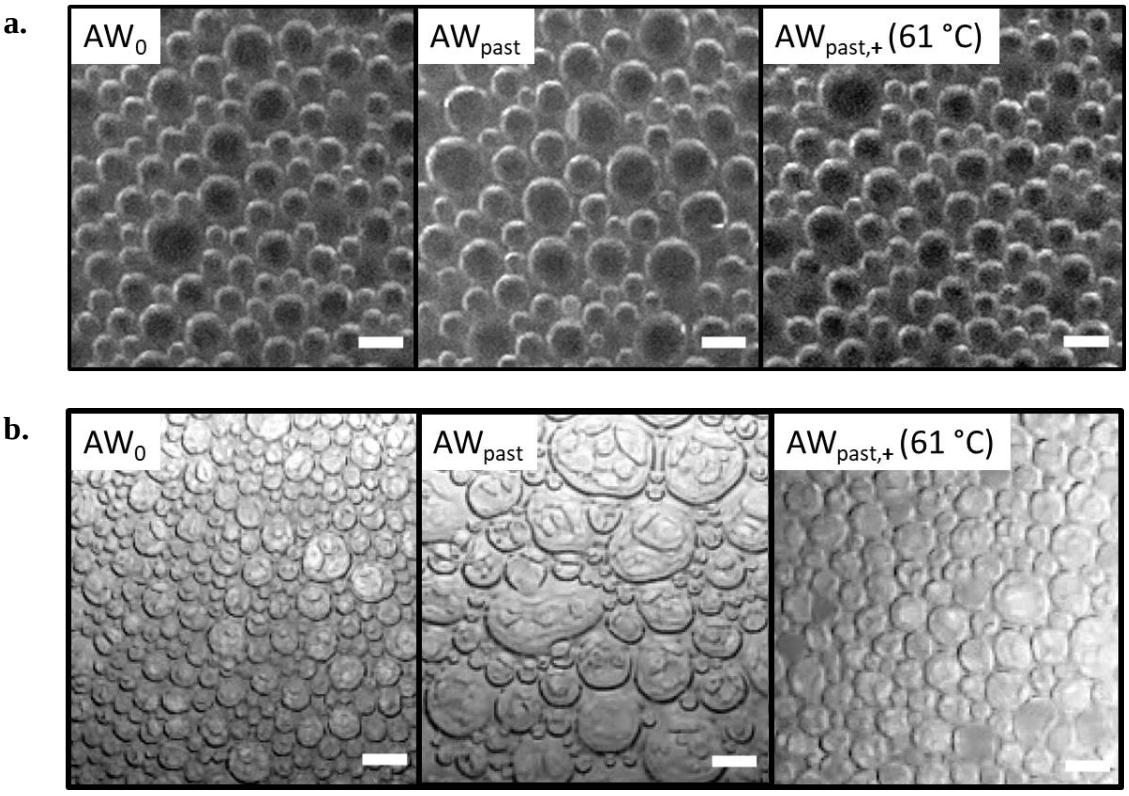

By Purwanti *et al.*
10.1016/j.idairyj/2022.105419

Figure 1. 2D-images of air bubbles in the fresh foam (a) and after half the volume of the entrapped liquid in the foam drained (b). The scale bar is 2 mm. By Purwanti *et al.*, 10.1016/j.idairyj/2022.105419 Figure 1

Revised on 30 April 2022; Accepted on 1 May 2022
Purwanti, N., Hogan, S. A, Maidannyk, V. A., Mulcahy, S., & Murphy, E. G. (2022). Effect of pasteurisation and foaming temperature on the physicochemical and foaming properties of nano-filtered mineral acid whey. *International Dairy Journal*, 133, 105419. doi: 10.1016/j.idairyj/2022.105419

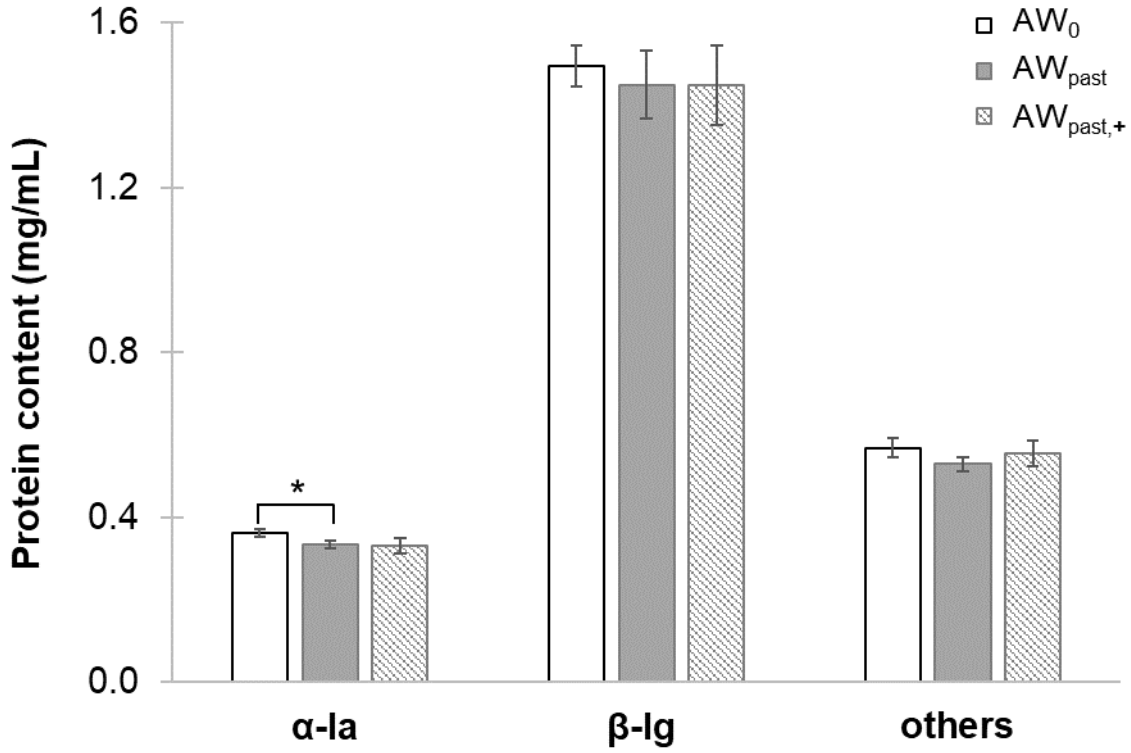

By Purwanti *et al.*
10.1016/j.idairyj/2022.105419

Figure 2. The remaining native α-la, β-lg, and other proteins in AW samples before pasteurisation (AW_0), after pasteurisation (AW_{past}) and after heat treatment at 61 °C ($AW_{past,+}$). * indicates a significant difference between the two AW samples ($p < 0.05$). By Purwanti *et al.*, 10.1016/j.idairyj/2022.105419 Figure 2

Revised on 30 April 2022; Accepted on 1 May 2022
Purwanti, N., Hogan, S. A, Maidannyk, V. A., Mulcahy, S., & Murphy, E. G. (2022). Effect of pasteurisation and foaming temperature on the physicochemical and foaming properties of nano-filtered mineral acid whey. *International Dairy Journal*, 133, 105419. doi: 10.1016/j.idairyj/2022.105419

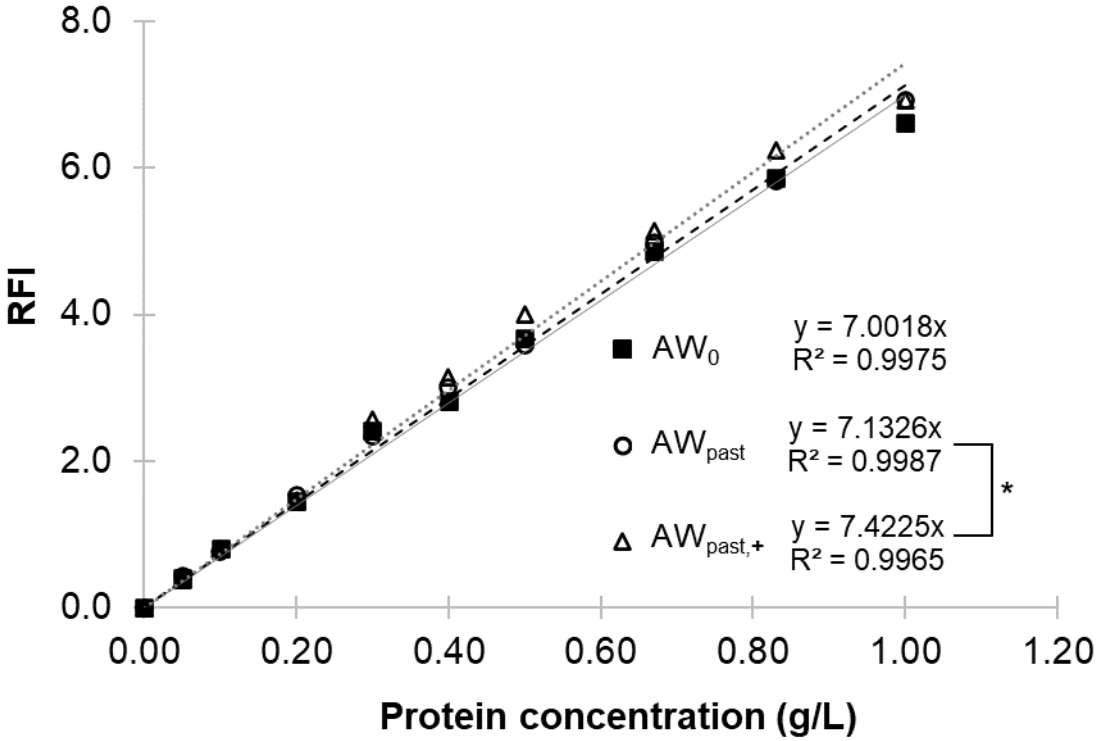

By Purwanti *et al.*
10.1016/j.idairyj/2022.105419

Figure 3. Relative fluorescence intensity (RFI) of AW as function of protein concentration. The degree of hydrophobicity is represented by the slope and * indicates a significant difference between AW samples. By Purwanti *et al.*, 10.1016/j.idairyj/2022.105419 Figure 3

Revised on 30 April 2022; Accepted on 1 May 2022
Purwanti, N., Hogan, S. A, Maidannyk, V. A., Mulcahy, S., & Murphy, E. G. (2022). Effect of pasteurisation and foaming temperature on the physicochemical and foaming properties of nano-filtered mineral acid whey. *International Dairy Journal*, 133, 105419. doi: 10.1016/j.idairyj/2022.105419

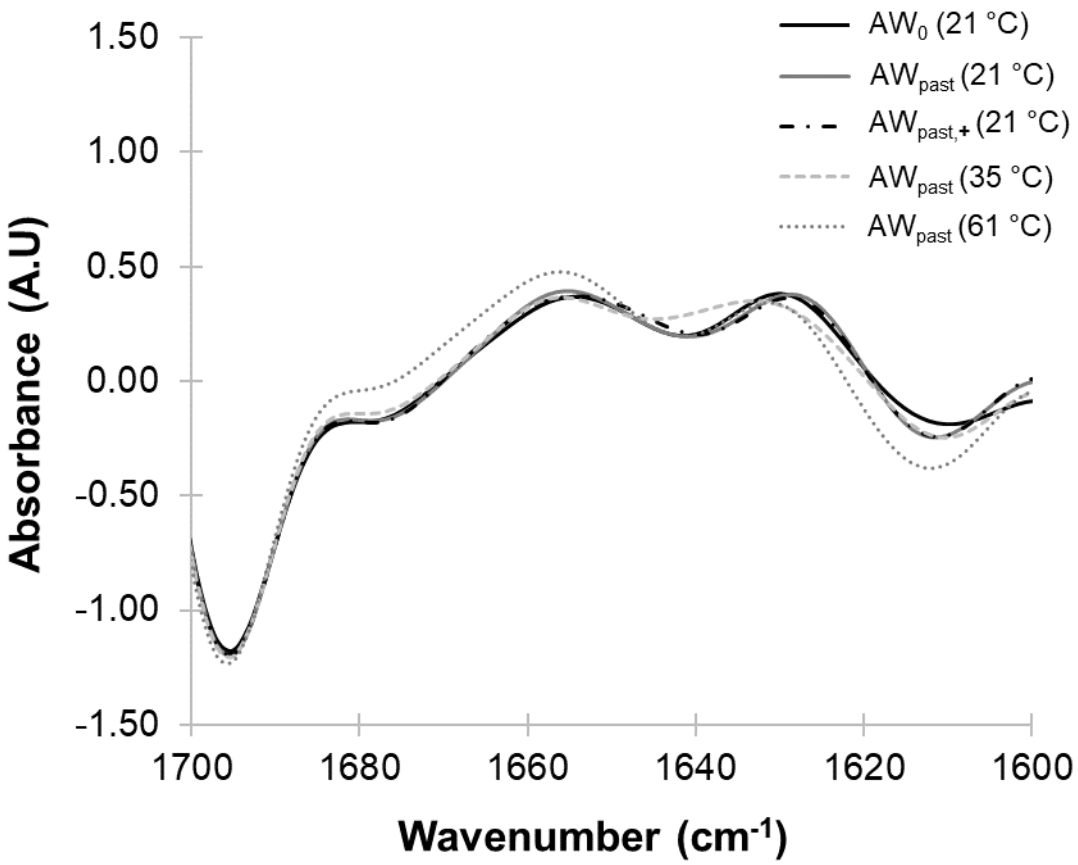

By Purwanti *et al.*
10.1016/j.idairyj/2022.105419

Figure 4. FTIR spectra (Amide I region) following normalization and deconvolution. By Purwanti *et al.*, 10.1016/j.idairyj/2022.105419 Figure 4

Revised on 30 April 2022; Accepted on 1 May 2022
Purwanti, N., Hogan, S. A, Maidannyk, V. A., Mulcahy, S., & Murphy, E. G. (2022). Effect of pasteurisation and foaming temperature on the physicochemical and foaming properties of nano-filtered mineral acid whey. *International Dairy Journal*, 133, 105419. doi: 10.1016/j.idairyj/2022.105419

a.

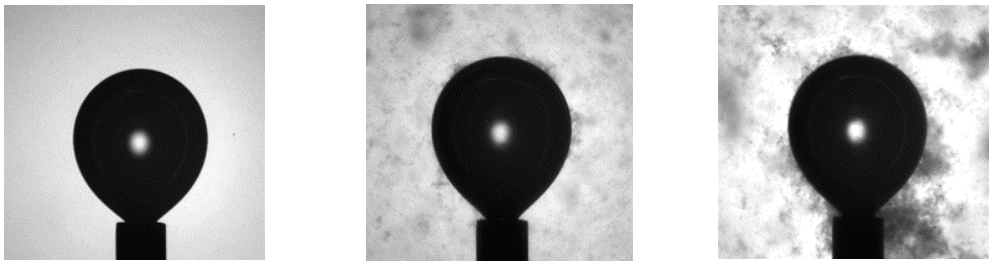

AW_0 AW_{past} AW_{past} (35 °C)

b.

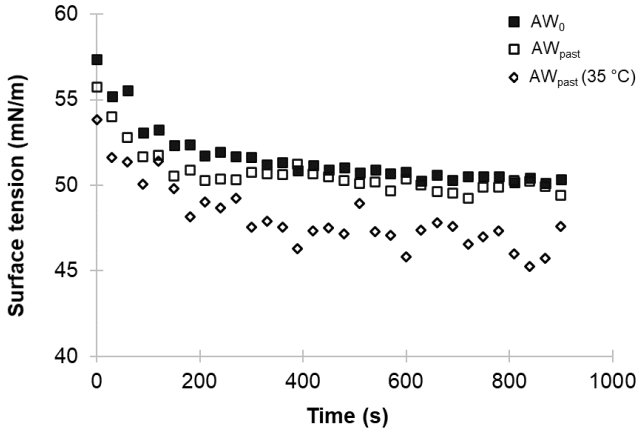

c.

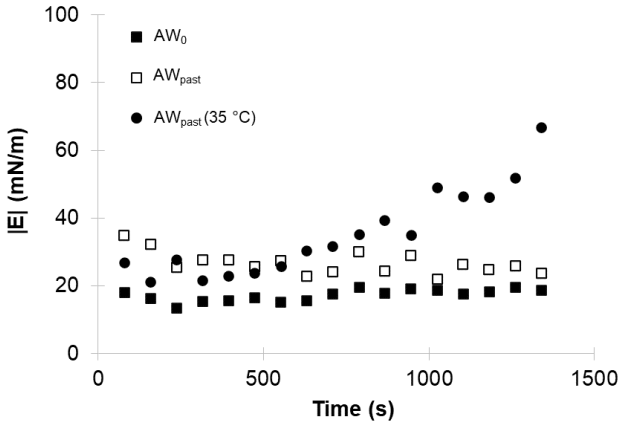

By Purwanti *et al.*

10.1016/j.idairyj/2022.105419

Figure 5. Tensiometer images of the air drop in AW_0, AW_{past} and AW_{past} (35 °C) at 0.1% w/w protein content during measurement of dynamic surface tension at 21 °C (AW_0 and AW_{past}) and 35 °C (AW_{past}) (a), surface tension as a function of time (b) and dilatational modulus as a function of time (c). By Purwanti *et al.*, 10.1016/j.idairyj/2022.105419 Figure 5

Revised on 30 April 2022; Accepted on 1 May 2022
Purwanti, N., Hogan, S. A, Maidannyk, V. A., Mulcahy, S., & Murphy, E. G. (2022). Effect of pasteurisation and foaming temperature on the physicochemical and foaming properties of nano-filtered mineral acid whey. *International Dairy Journal*, 133, 105419. doi: 10.1016/j.idairyj/2022.105419

a.

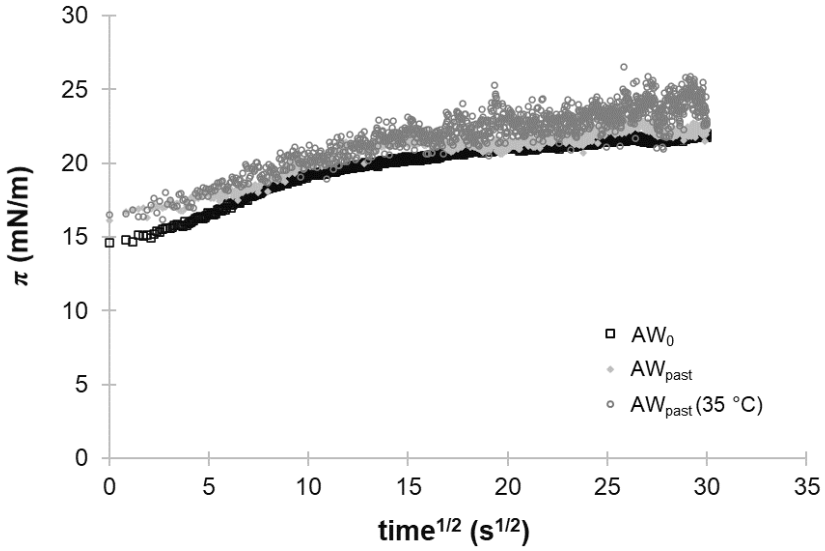

b.

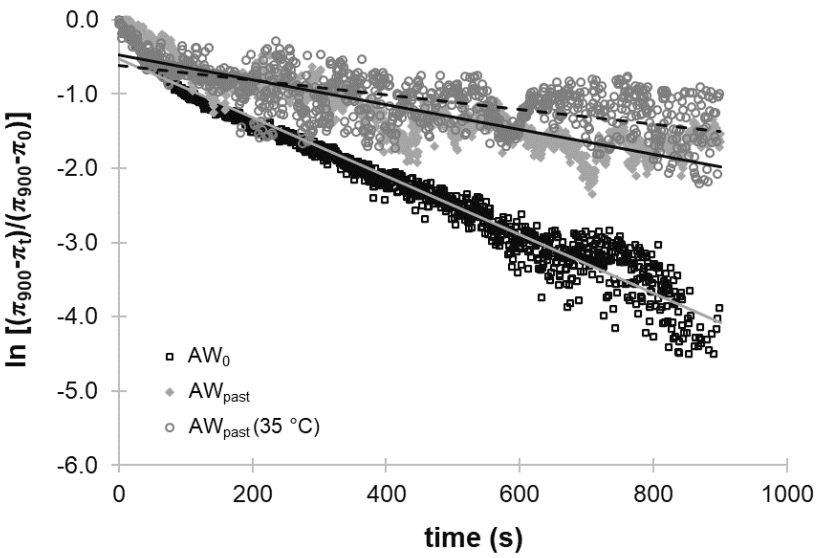

By Purwanti *et al.*

10.1016/j.idairyj/2022.105419

Figure 6. The average of the square root of time ($t^{1/2}$) dependence of surface pressure (π) (a) and representative of fit of first-order rate constant of adsorption and unfolding (b). By Purwanti *et al.*, 10.1016/j.idairyj/2022.105419 Figure 6

Revised on 30 April 2022; Accepted on 1 May 2022
Purwanti, N., Hogan, S. A, Maidannyk, V. A., Mulcahy, S., & Murphy, E. G. (2022). Effect of pasteurisation and foaming temperature on the physicochemical and foaming properties of nano-filtered mineral acid whey. *International Dairy Journal*, 133, 105419. doi: 10.1016/j.idairyj/2022.105419